REVIEW ARTICLE

Fast pressure-sensitive paint for understanding complex flows: from regular to harsh environments

Di Peng[1] · Yingzheng Liu[1]

Abstract

This review summarizes state-of-the-art knowledge on fast-responding pressure-sensitive paint (fast PSP), which has evolved into a powerful experimental tool for studying complex flow problems. As the formulation of porous paint with kilohertz response is now well established, full-field pressure measurements with high spatial and temporal resolution have been achieved on both stationary and moving targets. Recent studies have significantly advanced every aspect of this technology, including paint development, theoretical modeling, system integration and data processing. Novel paint formulations with superior sensing properties and additional functions for multi-physical measurements are being continually developed. The dynamic response mechanism is better understood through analysis and modeling considering the processes of photoluminescence, gas diffusion and light transmission. More importantly, applications of fast PSP are being expanded from regular wind-tunnel tests to more challenging conditions featuring hypervelocity, fast rotation and high temperature. Interdisciplinary research has played a key role in these development processes, and will remain vital for future breakthroughs in PSP technology.

Graphic abstract
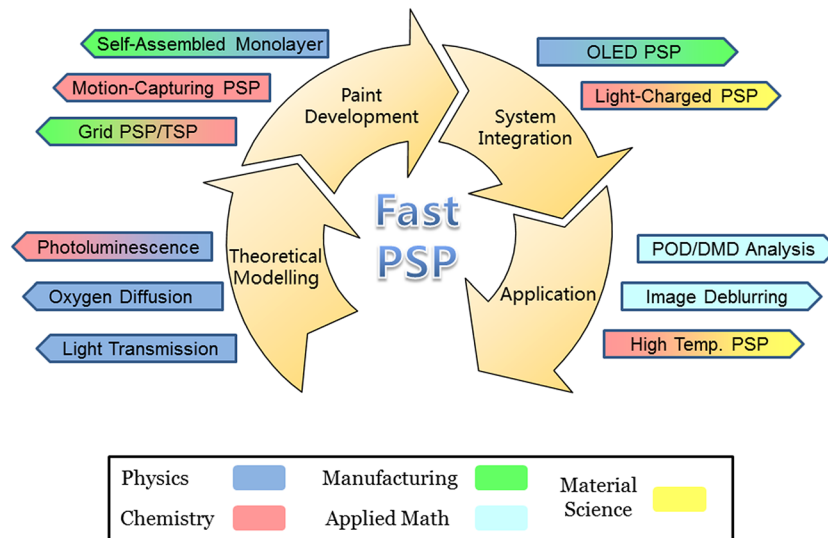
✉ Yingzheng Liu
yzliu@sjtu.edu.cn

[1] Shanghai Jiao Tong University, Gas Turbine Research
    Institute/School of Mechanical Engineering, 800 Dongchuan
    Rd., Shanghai 200240, China

List of symbols

A	Coefficient of Stern–Volmer equation
B	Coefficient of Stern–Volmer equation
D_m	Oxygen diffusion coefficient in PSP binder
d_{fr}	Fractal dimension of the porous binder
h	Paint thickness

|	
I	Intensity
I_0	Intensity at the beginning of luminescent decay
I_{G1}	Intensity of gate 1
I_{G2}	Intensity of gate 2
I_{ref}	Intensity at reference condition
P	Pressure
P_{ref}	Pressure at reference condition
Sa	Surface roughness
T	Temperature
T_0	Stagnation temperature
T_{ref}	Temperature at reference condition
t	Time
t_d	Test duration
ΔT	Temperature change
τ	Luminescent lifetime
τ_d	Time constant of oxygen diffusion
τ_{ref}	Luminescent lifetime at reference condition
ω	Angular velocity

1 Introduction

Pressure-sensitive paint (PSP), an optical method for full-field pressure measurement on model surfaces has found widespread applications in aerospace research since the 1980s. This technology entered a new era around 2000, due to the development of fast-responding pressure-sensitive paint (fast PSP) which enabled measurement with high spatial and temporal resolution. A variety of PSPs have been developed with response times of a few hundred microseconds or less, which could provide unsteady measurements at kilohertz frequencies with help from the fast evolving high-speed imaging technology. The time-resolved pressure fields yielded by fast PSP have afforded valuable insight into complex flow problems from vortex-induced noise/vibration

at low-speed to shock–boundary-layer interactions at high-speed. More importantly, fast PSP has made high-fidelity measurements and comprehensive diagnostics possible on helicopter rotors, engine compressors and hypersonic vehicle, whereas conventional pressure transducers usually underperform or even fail under these harsh conditions.

The theoretical basis and measurement techniques of PSP have been well documented by Liu et al. (1997), Bell (2001), and Liu and Sullivan (2005). Two recent review articles by Gregory et al. (2008, 2014a) have concentrated on fast PSP. In light of the literature, this review only briefly discusses the fundamentals of PSP technology. Instead, the main focus is to highlight the recent developing trends, which are: (1) advanced manufacturing techniques, which have enabled precise coating design and fabrication at micro- and nanoscales, showing promise for enhancing PSP's sensing performance and producing highly integrated systems; (2) understanding of the dynamic response mechanism, which has been greatly improved by considering the combined effects of luminescent decay, oxygen diffusion and light attenuation; and (3) advanced measurement methods, which have been developed and optimized for harsh test conditions featuring hypervelocity, fast rotation and high temperature.

Above all, the multidisciplinary nature of PSP technology has become increasingly prominent as recent advances have been fueled by contributions from different fields including physics, chemistry, manufacturing, material science and applied mathematics, as summarized in Fig. 1. Accordingly, the remainder of this review is organized as follows. Section 2 introduces the fundamentals of fast PSP, including its working principles, data acquisition methods and measurement uncertainties. Section 3 covers paint development, with a focus on fast-responding porous binders and novel multifunctional PSPs. Section 4 discusses the dynamic response mechanism involving both experimental and modeling

Fig. 1 Recent developments in fast PSP technology with contributions from different fields
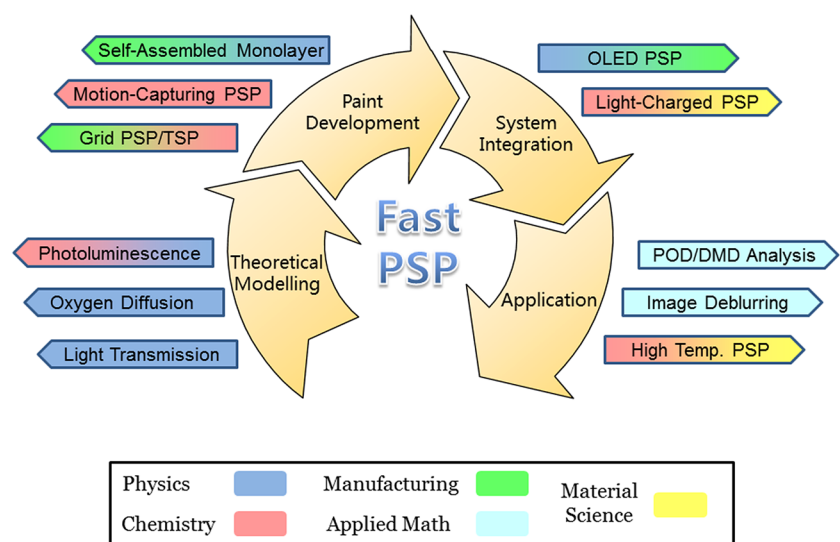
approaches. Section 5 presents the challenges and solutions as the use of fast PSP is extended from regular wind tunnel tests to harsh environments. The conclusion and outlook are given in Sect. 6.

2 Fundamentals of fast PSP

The working principle of PSP is based on molecular photoluminescence, where the luminescent molecules (i.e., luminophores) are firstly excited by an illumination source to a higher energy level, after which they return to their ground state, emitting longer-wavelength light in the process. The susceptibility of this emission process to surrounding environmental parameters (temperature, oxygen concentration, pH, etc.) has enabled the development of a rich class of optical sensors including PSP.

The mechanism of oxygen-quenching, a discovery made in the 1930s (Kautsky and Hirsch 1935), has served as the cornerstone of PSP measurement. Briefly, oxygen suppresses the emission process through its interaction with the excited luminophore, resulting in an inversely proportional relationship between oxygen concentration and luminescent intensity. A more straightforward explanation is available from the viewpoint of energy: for PSP, the energy absorbed from the excitation light will be consumed via three primary channels: light emission (i.e., luminescence), reaction with oxygen (i.e., oxygen quenching) and molecular collision (i.e., thermal quenching). At a constant temperature (with same energy loss due to collision), there is a direct competition between luminescence and oxygen quenching. Therefore, an increase in oxygen concentration leads to a reduction in luminescent intensity. The intensity of PSP can be further related to air pressure based on Henry's law, yielding the Stern–Volmer relation in the following form:

$$\frac{I_{ref}}{I} = A(T) + B(T)\frac{P}{P_{ref}}, \tag{1}$$

where I_{ref} and P_{ref} are the luminescent intensity and the air pressure at a reference condition, respectively. The temperature-dependent coefficients A and B are experimentally determined by calibration. In a typical wind tunnel application, a reference (wind-off) image is taken when the tunnel is off, and a wind-on image is taken when the tunnel is on. The reference image is necessary to remove the errors caused by the non-uniformity in illumination field and luminophore distribution. The intensity ratio of these two images can be converted to a pressure ratio according to Eq. (1), which then yields the pressure distribution (for a known reference pressure). This intensity-based method (also known as the radiometric method) is commonly used in PSP measurements, and requires a stable illumination source (e.g., an LED array) for excitation and a scientific-grade camera for data acquisition.

Alternatively, the Stern–Volmer relation can be expressed in terms of the luminescent lifetime of PSP. The typical response of PSP to pulsed excitation light follows a single exponential decay:

$$I(t) = I_0 e^{-t/\tau}, \tag{2}$$

where I_0 is the intensity at the start of the decay and τ is the lifetime of PSP. Then, the lifetime version of Stern–Volmer relation is:

$$\frac{\tau_{ref}}{\tau} = A(T) + B(T)\frac{P}{P_{ref}}, \tag{3}$$

where τ_{ref} is the luminescent lifetime at a reference condition. A photomultiplier tube (PMT) can accurately resolve the lifetime of PSP, but it is limited to point measurement. To achieve two-dimensional measurement, a viable method is to capture two (or more) images using a gated camera during the luminescent decay of PSP following excitation by a pulsed LED or a high-power laser. Theoretically, the intensity ratio of these two gates is directly related to surface pressure with no dependency on absolute intensity, thus eliminating the need for wind-off images (Holmes 1998; Goss et al. 2000). However, spatial variations in PSP lifetime still exist due to paint inhomogeneity (Ruyten et al. 2009), and the corresponding errors can be removed by taking a ratio of ratios with a reference image-pair (Gregory et al. 2009; Juliano et al. 2011). The resulting relation is:

$$\frac{\left(I_{G1}/I_{G2}\right)_{ref}}{I_{G1}/I_{G2}} = A(T) + B(T)\frac{P}{P_{ref}}, \tag{4}$$

where I_{G1} and I_{G2} are the time-integrated intensity images for gates 1 and 2, respectively. The lifetime-based method has shown clear advantages over the intensity-based method, as it is almost immune to errors related to model displacement or deformation (Schreivogel et al. 2012; Yorita et al. 2017). In particular, it has offered a valuable solution for PSP measurements on rotating blades of helicopter rotors and engine compressors (see the detailed discussion in Sect. 5.3). In addition, lifetime-based measurement can be performed using a frequency-domain technique, where sinusoidal light is generated for excitation and the PSP signal is recorded to calculate the pressure-dependent amplitude attenuation or phase shift (Holmes 1998). The recent development in frequency-domain fluorescence lifetime imaging (FLIM) technology has significantly lowered the technical barriers of this method, making it more accessible to industrial applications (Yorita et al. 2019).

The temporal response of conventional PSP is primarily governed by the thickness of the paint formulation (h) and

the diffusion coefficient of the binder material (D_m). The time constant of the paint response is given by:

$$\tau_d = \frac{h^2}{D_m}, \tag{5}$$

which indicates that a faster response can be achieved by either reducing the paint thickness or increasing the binder diffusivity. Although the former option is more appealing according to Eq. 5, it is actually less practical considering the trade-off which must be made between signal level and dynamic response (Schairer 2002). In reality, the prevailing method involves creating a porous binder to facilitate oxygen diffusion and enable immediate interaction between oxygen and luminophore (Sakaue et al. 2002a). In this way, the frequency response of PSP can easily reach a few kHz without sacrificing the signal-to-noise ratio (SNR). The two major types of porous paint used are polymer-ceramic PSP (PC-PSP) and anodized-aluminum PSP (AA-PSP), which will be described in Sect. 3.1, together with some novel configurations of fast PSP.

Measurement techniques for capturing unsteady pressure fields have evolved quickly, in accordance with the significantly enhanced frequency–response of PSP. The three primary methods are summarized in Table 1, based on the comparative study of Fang et al. (2012), including the phase-averaging method, the real-time method and the single-shot lifetime method. For the phase-averaging method, short light pulses are generated from the LED arrays, which are phase-locked with the surface pressure oscillations. PSP signals at one phase position are accumulated over many cycles by keeping the camera shutter open to achieve a high SNR (Singh et al. 2011). This method can be readily applied to situations involving periodic flow/pressure features if a proper trigger signal is available, such as flow over a cylinder (McGraw et al. 2006), fluid oscillator (Gregory et al. 2007), acoustic resonance chamber (Gregory et al. 2006) or impinging jet resonance (Davis et al. 2015). It should be noted that this method is susceptible to errors caused by frequency jitter or trigger-signal noise. Matsuda et al. (2013) proposed an alternative heterodyne method that could achieve unsteady measurement with a low frame-rate camera.

The real-time method uses a high-speed camera to directly capture the time-resolved PSP images, and has become increasingly popular due to the development of complementary metal oxide–semiconductor (CMOS) sensors for high-speed imaging technology. This method is the easiest of all three to implement, but has a fairly demanding hardware requirement including high-power, high-stability LED arrays and a sensitive high-speed camera. It is especially useful in shock tubes and hypersonic tunnels with short test durations on the order of milliseconds (Sakamura et al. 2005; Kameda et al. 2005). However, the measurement bandwidth is inherently limited due to the trade-off between sampling rate and signal level. The SNR at higher sampling rate can be improved by adopting a conditional image-sampling technique or a noise-removal technique based on principal component analysis (Pastuhoff et al. 2013; Peng et al. 2016c). It is also possible to use a phase-lock sampling method which allows direct phase-averaging treatment (Gardner et al. 2014). Still, the pressure resolution and SNR of a 12-bit CMOS camera is clearly inferior to those of a 14-bit or even 16-bit charged-couple device (CCD) camera, which creates difficulties in low-speed applications (Asai and Yorita 2011).

The single-shot lifetime method has been developed specifically to deal with the issues of model movement or deformation between wind-off and wind-on conditions, which are frequently encountered in applications involving fluid–structure interactions, helicopter rotors and turbomachinery. Typically, two consecutive images (G1 and G2) are taken by an interline transfer CCD camera on the luminescent decay of PSP following a pulsed excitation, and the transient pressure field is obtained using Eq. 4. The high-energy laser pulses afford a sufficient SNR within a single shot, thus eliminating the need for phase-averaging (Gregory et al. 2009; Juliano et al. 2011). Currently, the primary limitation of this method is the

Table 1 Comparison of unsteady measurement techniques using fast PSP

Method	Phase-averaging	Real-time imaging	Single-shot lifetime
Light source	Pulsed LED	Continuous LED (high power)	Pulsed laser (Nd:YAG, 532 nm)
Imaging device	CCD camera	High-speed CMOS camera	CCD camera with dual-exposure mode
Trigger signal required	Yes	No	Yes
SNR	High	Low	High
Pressure resolution	High (up to 16-bit)	Low (up to 12-bit)	Moderate (up to 14-bit)
Typical application	Stationary model in low-speed periodic flow	Stationary model in complex flow with multiple frequencies	Model with motion and/or deformation
Major error source	Temperature effect, model motion/vibration, photodegradation	Temperature effect, model motion/vibration, photodegradation, camera noise	Temperature effect, image misalignment and blur

operating frequency of high-power Nd:YAG laser, which is usually < 20 Hz.

The primary sources of error for each of the above three measurement techniques are presented in Table 1. While the detailed error-analysis of conventional PSP measurement in early literature still applies for fast PSP (Liu et al. 2001a; Liu and Sullivan 2005), some later modifications warrant comment. Undoubtedly, the temperature-induced error remains the most significant for all methods, and is actually exacerbated by the high temperature-sensitivity of fast PSPs. The luminophores deposited on the open structure of porous binders are directly exposed to the outer environment, and thus more susceptible to temperature variations. For a typical PC-PSP with a pressure sensitivity of 0.7%/kPa and a temperature sensitivity of 2.4%/K, a 1 K change in temperature would lead to a pressure error of over 3 kPa (Peng and Liu 2016). The temperature-induced error is less for AA-PSP, but is still exceeds 1 kPa/K (Merienne et al. 2015). Usually, errors caused by a bulk temperature change between wind-on and wind-off conditions can be effectively removed through the application of in situ calibration. If a complex temperature-distribution is present on the model surface (which is common in high-speed and engine-related applications), it is important to acquire the temperature map via other techniques (temperature-sensitive paint, infrared thermography, etc.) and subsequently perform temperature correction on PSP data. For the intensity-based methods (phase-averaging and real-time), other noticeable error sources include the illumination variation caused by model movement or vibration, and the photodegradation of PSP. In particular, the photodegradation effect cannot be neglected even for the real-time measurement with a fairly short data-acquisition time. This is due to the porous paint degrading much faster than its steady-state counterpart (Matsuda et al. 2016; Panda 2017) and the continuous high-power excitation further accelerating the photodegradation process (Merienne et al. 2012). The corresponding temporal variations in intensity can be compensated by normalizing the images using a fitted curve (Panda 2017; Jiao et al. 2018a). Camera noise is also a significant source of interference for real-time measurement, especially at the high sampling-rates when signal levels are otherwise insufficient; this problem can be alleviated as previously discussed. For the single-shot lifetime method, the error sources (aside from the temperature effect) are mostly related to model motion and deformation, such as image-registration errors and image blur. The effects of these errors can be minimized by the development and use of advanced image-registration and deblurring algorithms (Juliano et al. 2012; Disotell et al. 2014).

3 Paint design and fabrication

3.1 Binder development

The key component of fast PSP is its porous binder, which allows rapid oxygen diffusion and thus a fast response. Typically, such a porous binder can be created via the following two methods: (1) suspending ceramic particles (TiO_2, SiO_2, etc.) and a small amount of polymer in an appropriate solvent, and air-spraying the resulting slurry onto the model surface to form a porous coating (Scroggin et al. 1999; Gregory et al. 2006; Sakaue et al. 2011); and (2) performing anodization on an aluminum model to form a porous structure on the surface (Sakaue 1999; Kameda et al. 2004). These two methods, referred to as polymer-ceramic PSP (PC-PSP) and anodized-aluminum PSP (AA-PCP), afford PSPs with a frequency response of several kHz or greater.

PC-PSP can be easily air-sprayed on test models, regardless of the material from which these models are made, or their geometry. However, this means it is difficult to precisely control the physical properties of the PSPs (thickness, surface roughness, etc.) which affect its sensing performance (Pandey and Gregory 2016; Jiao et al. 2018b). In contrast, the fabrication process of AA-PSP can be tightly controlled, and thus produce PSPs with highly reproducible physical properties and allow further improvements in sensing performance (Sakaue and Ishii 2010a, b). In particular, the size and depth of the pores can be controlled by the anodization parameters (temperature, voltage, duration, etc.), and extremely short response times (< 1 μs) can be achieved with large and shallow pores (Fujii et al. 2013). Unfortunately, the requirement for anodization does restrict the application of AA-PSP to aluminum models with relatively simple geometry and limited size. As shown in Fig. 2, while recent research activities have focused on improving the sensing performance of both PC-PSP and AA-PSP, a number of novel fast PSPs were also introduced through advanced manufacturing techniques.

In PC-PSP, the luminophore [typically PtTFPP or Ru(dpp)$_3$] can be deposited by dipping the binder into luminophore solution, by overspraying luminophore solution on the binder surface or by pre-mixing luminophore with the binder slurry (before spraying). The choice of deposition method is critical because it determines the luminophore distribution inside the binder and thus greatly affects the dynamic response. The first two deposition methods (dipping and overspraying) generally result in a luminophore distribution near the binder surface, which enables immediate interaction between oxygen and luminophore, affording a response time within 100 μs (Hayashi
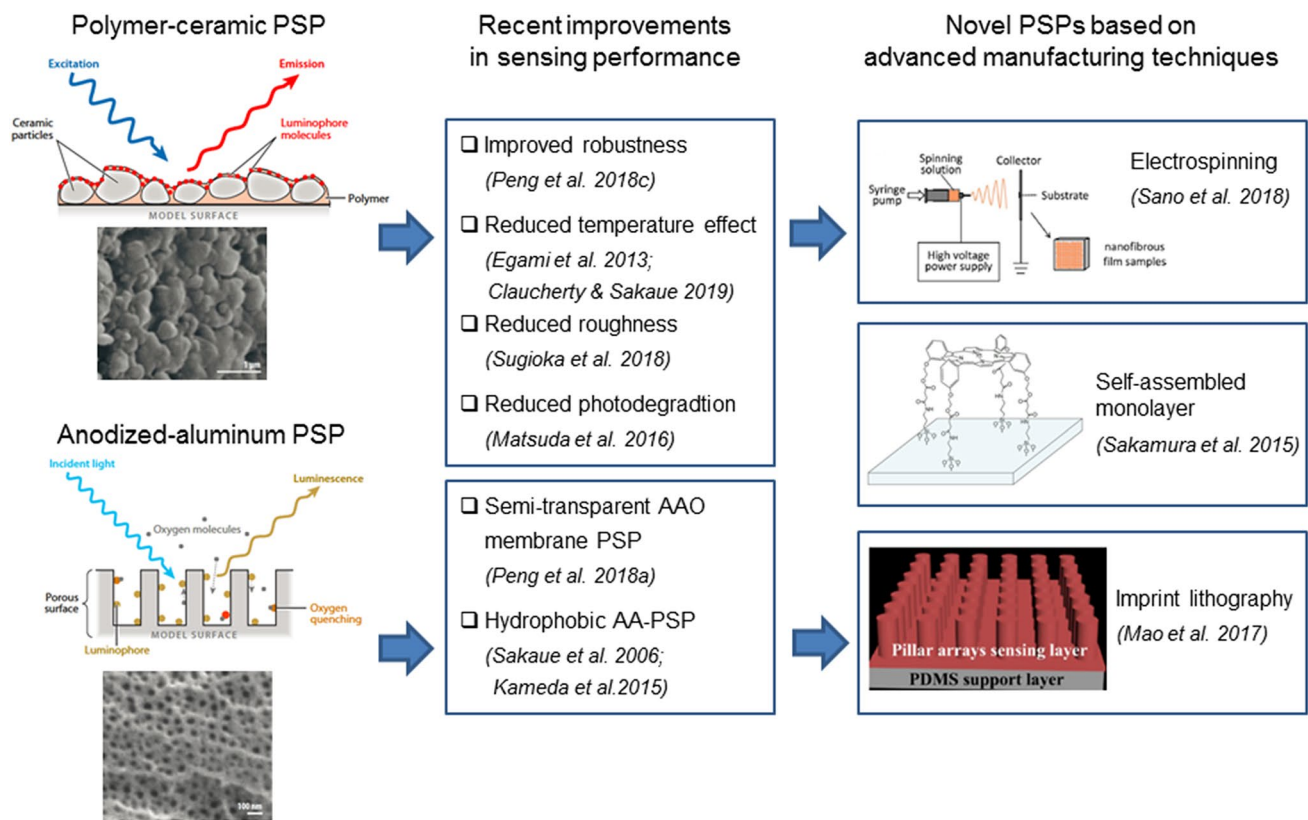
Fig. 2 Recent advances in paint development of fast PSP

and Sakaue 2017; Egami et al. 2019a). As the polymer portion in porous binders usually has a low oxygen diffusion rate, its concentration should be well controlled to ensure a fast response (Sakaue et al. 2011). The delaying effect of polymer can be reduced by adopting a particle/dye-absorb method, in which the mixture of dye and particles is adsorbed onto a polymer-coated film (Sugioka et al. 2018a). In contrast, the third deposition method produces a relatively uniform luminophore distribution throughout the binder, which leads to a slower response, since oxygen takes a longer time to reach and interact with luminophores in the bottom layer (Klein et al. 2007; Li et al. 2018). A response time of less than 100 μs can be achieved by applying a fairly thin layer of coating (5–10 μm) with no addition of polymer (Kameda et al. 2012). However, the improvement in dynamic response is often accompanied by reduced paint durability. For example, coatings with near-surface luminophore distribution were found to be quite susceptible to mechanical damage in high-speed applications (Lo and Kontis 2016; Peng et al. 2016b). Reduction in thickness and polymer concentration would further compromise the coating's mechanical strength.

To resolve this conflict, a new formulation of fast PSP was developed using mesoporous, hollow SiO_2 particles as luminophore hosts to provide additional paths for oxygen diffusion. This mesoporous-particle-based PSP (MP-PSP) featured both fast response (~ 100 μs) and high durability with a uniform luminophore distribution over a thickness of 50 μm (Peng et al. 2018c). The response time could be reduced to 5 μs or less for a paint with a similar formulation and thickness of 2–3 μm, as shown by Egami et al. (2019b). In addition, efforts were made to enhance the performance of PC-PSP and minimize possible measurement errors. Egami et al. (2013) used highly thermal-conductive particles (e.g., boron nitride) in paint binder to reduce temperature effects. Claucherty and Sakaue (2019) demonstrated a pyrene-based PC-PSP with low temperature sensitivity. Sugioka et al. (2018b) developed a PC-PSP with reduced surface roughness (~ 0.5 μm) for measurements in transonic flows. Matsuda et al. (2016) reported a PC-PSP based on polymer particles with high photostability.

For AA-PSP, the standard procedure is to apply $Ru(dpp)_3$ to the porous binder (after anodization) via dipping–deposition. The overspraying method has also been attempted, resulting in higher intensity but lower pressure sensitivity (Zare-Behtash et al. 2012). As previously stated, the primary concern of AA-PSP is its limited application due to the strict demands of base material and treatment technique. A recent study showed that this technical barrier could be overcome by using through-hole anodized-aluminum oxide

(AAO) membrane as the PSP binder (Peng et al. 2018a). A porous membrane with a thickness less than 100 μm was fabricated from an aluminum sheet via two-step anodization and chemical etching (Matsuda and Fukuda 1995; Schneider et al. 2005). This PSP membrane showed similar sensing properties to conventional AA-PSP, and it could be directly attached to the model surface for measurement. A further benefit is that the membrane's high transparency would enable measurements with back-illumination and back-imaging, which could be useful in certain cases with limited optical access. AA-PSP is also susceptible to humidity effects due to the hydrophilic nature of its porous surface. The pore contains electrolyte anions with a high charge density, which enables the easy physisorption of water molecules (Dickey et al. 2002). It was found that the intensity of PSP increased with relative humidity, while the pressure and temperature sensitivity remained unaffected. This humidity effect can be reduced by applying a hydrophobic mono-coating on top of the AA-PSP (Sakaue et al. 2006; Kameda et al. 2015).

In recent years, a number of advanced manufacturing techniques have been introduced to PSP fabrication for precisely controlling the physical properties while improving the sensing properties. Sakamura et al. (2015) adopted a self-assembled monolayer (SAM) technique to create ultra-thin PSP film on solid surfaces for microfluidic applications.

This SAM technique could be easily applied to a non-flat surface, showing advantages over the previously developed Langmuir–Blodgett (LB) deposition technique (Matsuda et al. 2011). In addition, techniques such as imprint lithography and electrospinning have been adopted to fabricate a highly porous binder that could effectively improve the pressure sensitivity of PSP (Mao et al. 2017; Sano et al. 2018).

3.2 Multi-functional fast PSPs

As fast PSP is now being used in challenging conditions involving hypervelocity and fast rotation, hybrid coatings with dual-sensing capability are highly desirable to counteract the measurement errors induced by temperature effects and model motion. It is also important to acquire temperature or deformation field simultaneously (with pressure) to investigate the strong coupling effect between these parameters. Meanwhile, a novel class of PSP integrating luminescent coatings with a light source is being developed, which may be especially valuable in engine-related applications with limited optical access. Those recent advances are summarized in Fig. 3, and then reviewed in this section.

Simultaneous pressure and temperature measurements can be achieved by combining PSP with temperature-sensitive paint (TSP) to give one of the following three
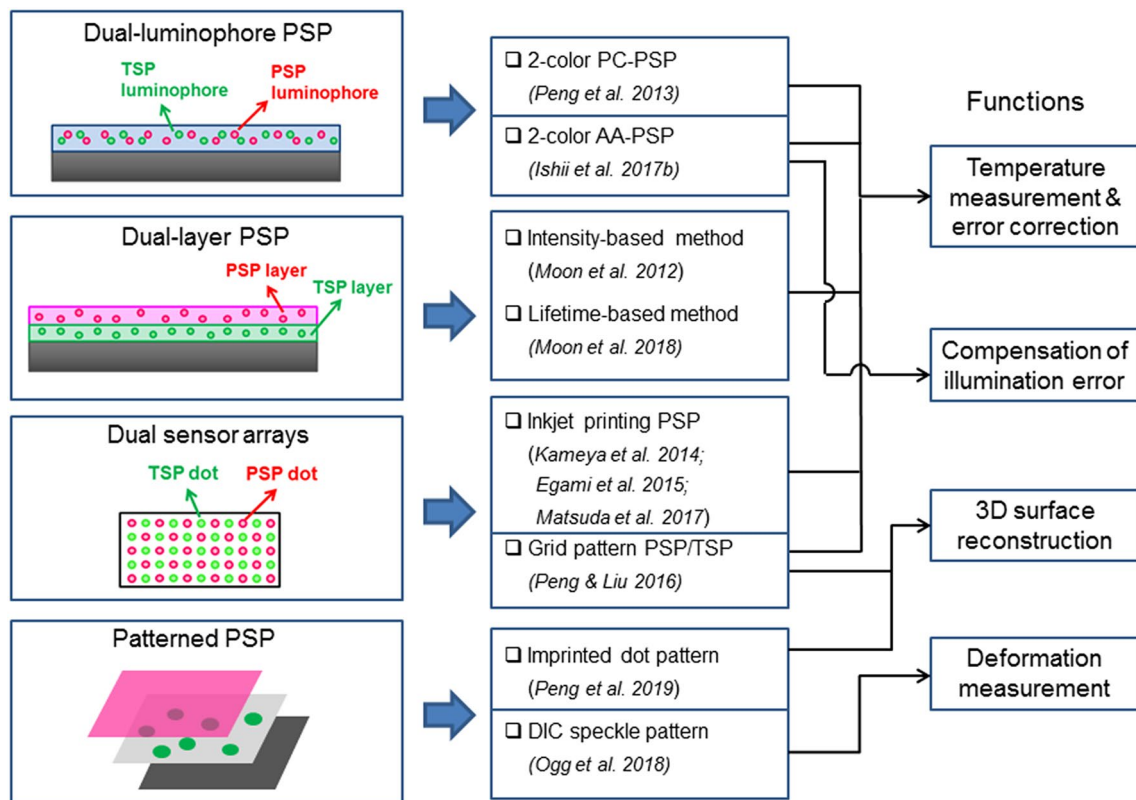

Fig. 3 Major types of multi-functional PSP

configurations: multi-luminophore paint, multi-layer paint and multi-sensor arrays. A multi-luminophore paint is fabricated by mixing two or more different luminophores into the same binder, which usually contains a PSP channel and a TSP channel. These channels have similar absorption spectra but distinct emission spectra, and the signals are captured by either a color camera or a camera with a filter-wheel system (Fischer et al. 2012). Dual-luminophore fast PSPs based on polymer/ceramic and anodized-aluminum binders were developed by Peng et al. (2013) and Ishii et al. (2017b), respectively. The main issue here is the spectral interference between the PSP and TSP channels due to the luminophore's broad emission band, which reduces the pressure sensitivity of the PSP channel and induces unwanted pressure sensitivity in the TSP channel. It is also important to ensure a uniform luminophore distribution, to minimize measurement errors due to sensitivity cross-talk.

An alternative configuration of a combined PSP/TSP system is achieved by multi-layer paint, in which pressure and temperature sensors are physically separated and confined within their own layers. The TSP layer incorporating an oxygen-impermeable binder lies on the bottom, while the PSP layer is on top to facilitate its interaction with oxygen. Between these PSP and TSP layers is an insulation layer, which prevents mixing and energy-transfer (Hyakutake et al. 2009; Moon et al. 2012). To resolve the problem of spectral interference, a dual-layer paint with temporally separated emissions was recently developed for lifetime-based measurement using a monochrome camera (Moon et al. 2018). The remaining problems include signal attenuation of the TSP layer and temperature correction errors (due to the temperature difference between PSP and TSP layers).

The third type of combined PSP/TSP system is the dual-sensor array, in which PSP and TSP dots are arranged alternately in close proximity. Inkjet printing was found to be an effective method for depositing these arrays on porous binders, such as a thin layer chromatography (TLC) plates and anodized-aluminum (Kameya et al. 2014; Egami et al. 2015). It was further found possible to use a commercial printer to fabricate complex patterns with high spatial resolution onto filter paper coated with a layer of poly(4-*tert*-butyl styrene) (Matsuda et al. 2017). A grid PSP/TSP system was also developed, consisting of PSP dot-arrays atop a TSP layer (Peng and Liu 2016). This sensor array configuration has the advantage of requiring only a monochrome camera for data acquisition, and is immune to both luminophore interaction and spectral interference; however, these advantages come at the cost of spatial resolution.

Several different formulations of multi-functional PSP have been developed for measurements on deforming and moving objects. A dual-luminophore (or binary) PSP with a pressure-insensitive reference dye is the common means of compensating for illumination errors due to model movement and deformation. Ideally, if the PSP and reference channels have identical temperature-sensitivity, the resulting intensity ratio should only be a function of pressure, which is unaffected by any illumination variation due to relative motion between the model and the light source (Crafton et al. 2013). A motion-capturing PSP system was developed by applying this idea to porous PSP with TLC and AA binders (Sakaue et al. 2013a; Ishii et al. 2017b), and was later tested on moving objects (Chin et al. 2017; Ishii et al. 2017a). This method can also remove errors due to light-contamination of plasma radiation in certain test environments (Hayashi et al. 2018).

For applications involving flow-structure interaction and aeroelasticity, simultaneous measurements of pressure and deformation are highly desirable. This can be achieved by the previously mentioned grid PSP with a two-camera lifetime system, assuming that the PSP dot-arrays can provide a basis for 3D surface reconstruction based on binocular vision (Peng et al. 2016a). If the PSP dots form a random pattern instead, they can serve as features for an image-stitching operation and resolve the key problem of limited view-angle in endoscopic PSP systems (Peng et al. 2019b). Alternatively, simultaneous measurement of pressure and deformation can be achieved by merging the digital image correlation (DIC) technique with binary PSP, While the PSP coating itself can provide patterns for DIC measurement, applying a traditional DIC pattern (black speckles) on top of PSP was found to be optimal for a reliable measurement of deformation (Ogg et al. 2018).

PSP integrated with the light source is a special type of multi-functional PSP which has emerged in recent years, and combines the functions of illumination- and pressure-sensing. This technique has the following benefits: (1) a greatly improved uniformity of illumination; (2) a simplified optical set-up, partly resolving the problem of limited optical access; (3) a model motion/deformation-independent illumination field, which prevents errors in intensity-based PSP measurements. As shown in Fig. 4a, such a system was initially realized by embedding a thin-layer electroluminescent (EL) device or organic light-emitting device (OLED) between the coating and the model surface to form a laminated PSP (Schulz and Klein 2005; Iijima and Sakaue 2011; Peng et al. 2018b). An alternative solution was proposed by Matsuda et al. (2012), in which the PSP luminophores were mixed into the emissive layer of OLED (see Fig. 4b). More recently, a light-charged PSP system was developed by merging the PSP luminophore with persistent luminescent (PL) phosphor (Peng et al. 2018d). As shown in Fig. 4c, the PL phosphor restores energy during the charging phase, and then produces a long afterglow as the excitation for PSP. This system can thus operate without any physical light source. It should be noted that the above techniques are in the early stages of development, with difficulties in

Fig. 4 Integration of PSP with light source: **a** laminated OLED-PSP, **b** mixed OLED-PSP, **c** light-charged PSP
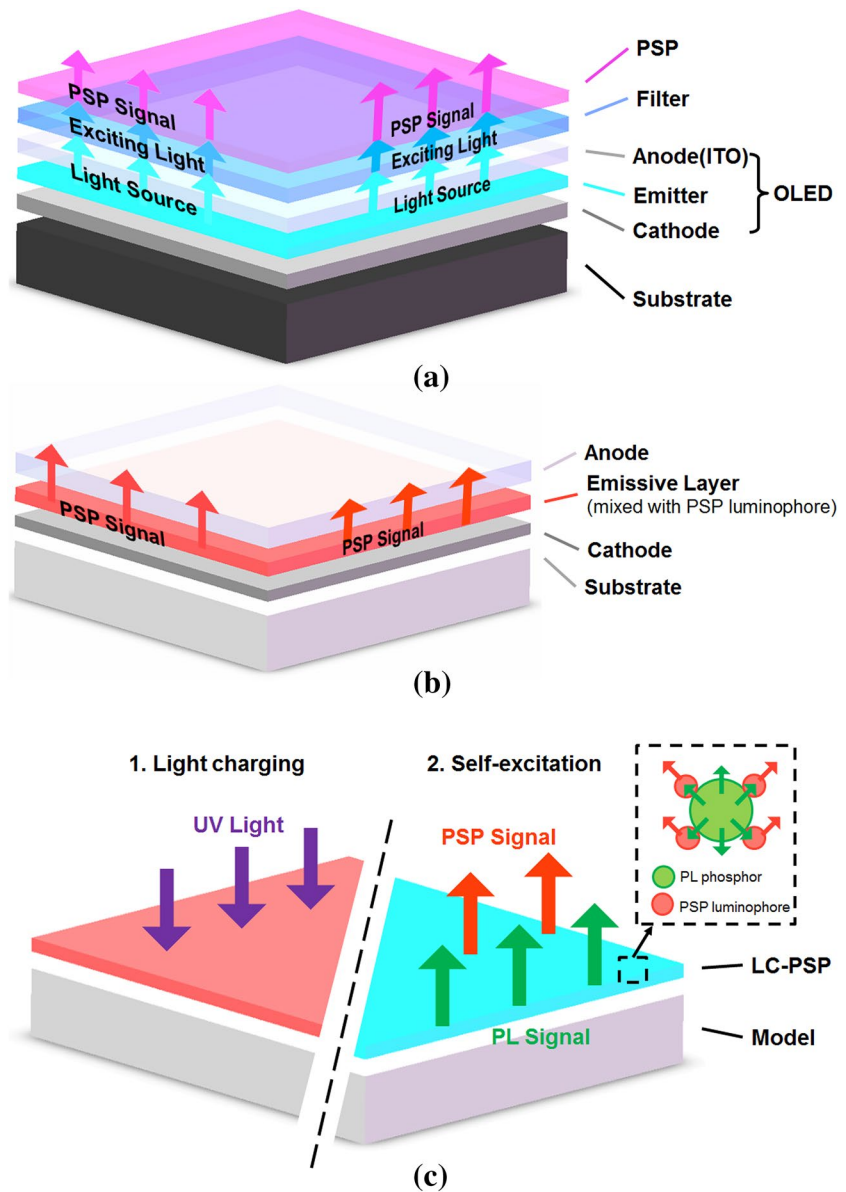
fabrication and implementation yet to be overcome. Nonetheless, they have shown decent prospects for future development and application.

4 Mechanism of dynamic response

The dynamic response is critical for fast PSP since it determines the measurement bandwidth. Theoretically, it is governed by both the intrinsic luminescent lifetime of the luminophore and the extrinsic diffusion timescale of oxygen within the binder. For conventional PSP, the effect of luminescent lifetime is negligible because it is a few orders of magnitude less that the gas-diffusion timescale (Kameda et al. 2004; Liu and Sullivan 2005). However, the porous

binder of fast PSP provides an oxygen diffusion timescale of down to 10 μs, which is close to the luminescent lifetime. Therefore, selecting a luminophore with a short lifetime is as important as increasing the gas diffusion rate for further improvement of PSP's dynamic response (Sakaue et al. 2013b; Gregory et al. 2014a).

The experimental methods for dynamic calibration have matured, as detailed in previous review articles (Gregory et al. 2008, 2014a). With use of calibration devices such as shock tubes (for step–response) and acoustic resonance tubes (for frequency–response), recent developments have focused on numerical methods for modeling the PSP's dynamic response, which could provide more insights about the underlying mechanism. Figure 5 presents the strategy for dynamic modeling of PC-PSP, which has yielded reasonable
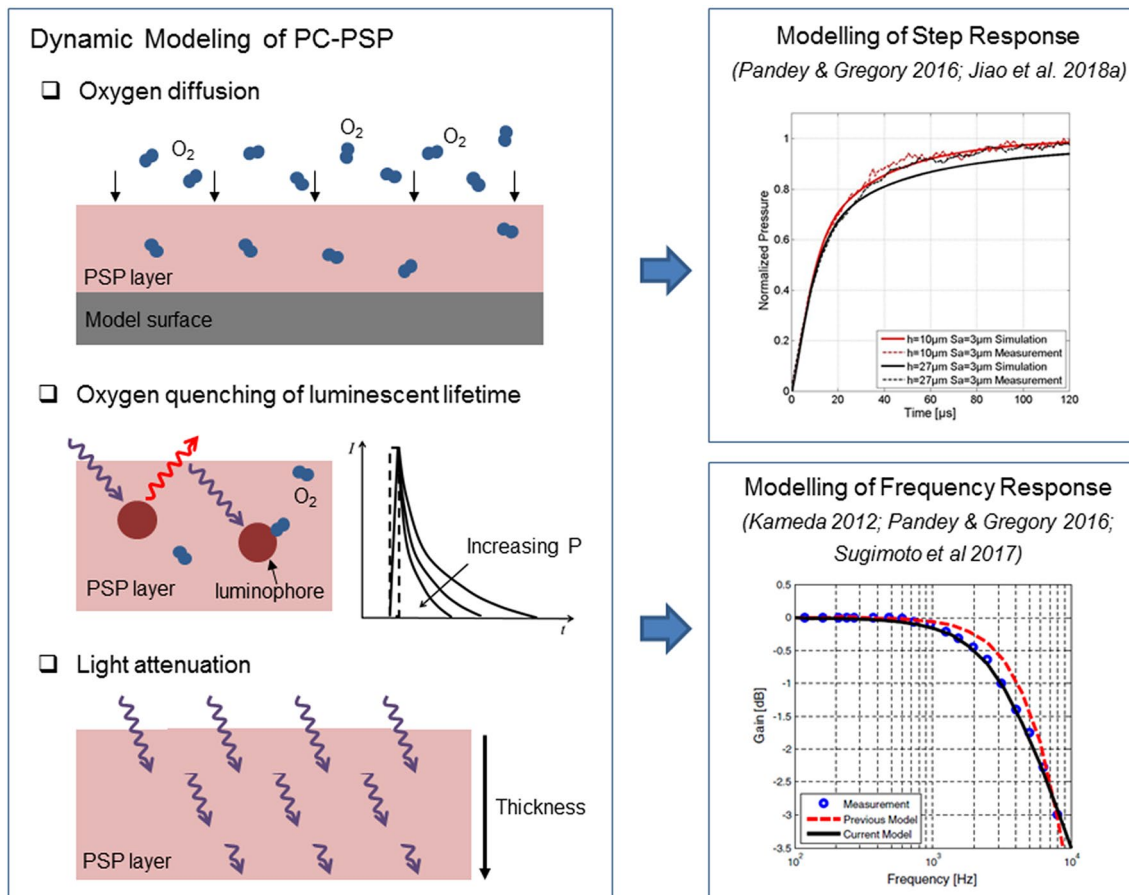
Fig. 5 Dynamic modeling of PC-PSP: method and application

predictions of both step–response and frequency–response. A detailed discussion about the current state of experimental and numerical methods is given below.

4.1 Step response

The step–response calibration device contains a shock tube, a continuous light source, a PMT and an oscilloscope. The paint response following the passage of a shock wave is captured by the PMT and recorded on the oscilloscope. Even though the response curve should theoretically be that of a more complicated system, it is generally accepted that it can be fitted using a first-order system, and the time-response is characterized by a single value of the 90% rise-time (Sakaue et al. 2002a, 2013b).

By considering the gas diffusion process inside the polymer binder, a classical square-law relation for the diffusion timescale can be obtained, as shown in Eq. (5). However, this solution does not hold for fast PSP with a porous binder, because the diffusion problem for a porous binder must be evaluated based on a two-phase system, comprising one disperse phase and one continuous phase. The mathematical

expression for this was derived by Liu et al. (2001b) as follows:

$$\tau_d = \frac{h^{2-d_{fr}}}{D_m},\qquad(6)$$

where d_{fr} is the fractal dimension of the pores, which is essentially a measure of the complexity of the pore pathway. Hayashi and Sakaue (2017) reported that the d_{fr} values of PC-PSP and AA-PSP were 1.8 and 1.5, respectively. Figure 6 shows the relation between response time and paint thickness for different formulations of PC-PSP and AA-PSP reported in previous studies. While the AA-PSP data can be roughly fitted to a straight line (except for the bottom ones with significantly larger pores), the PC-PSP data are highly scattered, due to the random pore structure and complex interactions between particle, polymer and solvent.

To accurately simulate the dynamic response of fast PSP, both oxygen diffusion and luminescent lifetime should be considered. An analytical model accounting for both factors was proposed by Kameda (2012), in which the one-dimensional diffusion of oxygen into PSP binder and the first-order

Fig. 6 Dependency of response time on paint thickness for different formulations of fast PSP
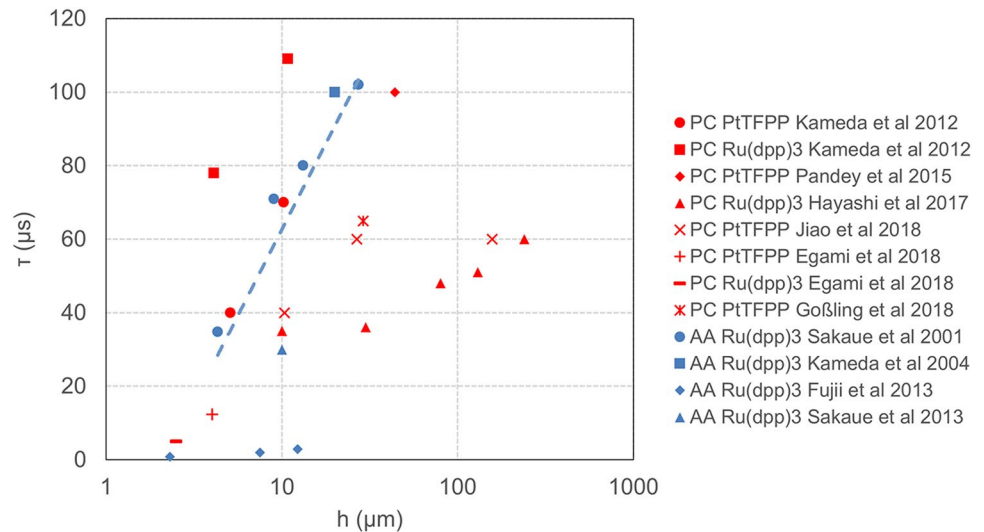
population dynamics of excited-state luminophores were implemented. In a subsequent work by Pandey and Gregory (2015), this model was improved to account for light attenuation and heterogeneity of the paint layer. Numerical simulation was performed for PC-PSP, on the assumption that the coating could be treated as a two-layer structure with a high diffusion rate in the rough top layer and a low diffusion rate underneath it. The simulation results matched the data from the experimental calibration, in terms of the effects of luminescent lifetime and surface roughness on dynamic response. In addition, the step–response varied with both amplitude and direction of the pressure change, due to the non-linear nature of the Stern–Volmer equation previous discovered by Gregory and Sullivan (2006). Later, this model was further developed to account for the paint-thickness effect (Jiao et al. 2018a) whereby oversprayed luminophore permeates into the binder and results in an effective thickness of around 15 μm, meaning that the effects of both surface roughness and coating thickness should be considered for a thin coating (≤ 15 μm).

4.2 Frequency response

The frequency response of fast PSP can be calibrated using an acoustic resonance tube with similar illumination and data acquisition devices to those used for step–response measurement. Standing waves are generated inside the tube by a speaker for a series of frequencies, and the amplitude/phase information of the PSP response is obtained by comparing the luminescent signal (from PMT) with the signal of a reference Kulite transducer. The PMT signal must be passed through an analog filter to improve its SNR. Currently, reliable measurement of frequency response is restricted to 10 kHz or less, mostly due to the physical

difficulties inherent to creating strong and repeatable fluctuations at higher frequencies.

It was initially found that the first-order system (based on luminescent lifetime only) could provide a good fit to the frequency response curves (Sugimoto et al. 2012). However, a more accurate fit was obtained by considering both the effects of lifetime and diffusion (McMullen et al. 2013). In fact, if the lifetime is much greater than the diffusion time-scale, the effect of lifetime dominates and the paint behaves similarly to a first-order system; if the lifetime is small compared to the diffusion time scale, the effect of diffusion dominates, approximating the behavior of a half-order system (Sugimoto et al. 2017). To further understand the frequency response mechanism of PC-PSP, numerical simulations were conducted using the analytical model mentioned in the previous section (Kameda 2012; Pandey and Gregory 2016). This allowed detailed examination of the effects of several key factors, including luminescent lifetime, light transmittance and surface roughness.

5 Measurement methods for challenging environments

Fast PSP measurement in a conventional high-speed wind tunnel is fairly straightforward when using an up-to-date system featuring a high-power LED and a high-speed camera, as already demonstrated by a number of studies using AA-PSP (Nakakita et al. 2012; Merienne et al. 2013, 2015) and PC-PSP (Bitter et al. 2012; Flaherty et al. 2014; Crafton et al. 2015; Panda 2017). The real challenges emerged as test conditions were being extended to study hypersonic flow, helicopter rotors, turbomachinery and aero-acoustics. Some representative cases were covered in the previous review article by Gregory et al. (2014a), which highlighted the

primary advantages of fast PSP for capturing and understanding complex flow phenomenon. Given the rapid evolution of measurement techniques in the past few years, a systematic overview will be given here for each of the following four categories: low-speed flow, hypersonic flow, fast-rotating blades and high-temperature environments.

5.1 Low-speed flow

Full-field high accuracy measurement of surface pressure-fluctuation is invaluable for turbulence and aero-acoustic research. Fast PSP is now a very promising method, as high-speed imagers have become increasingly accessible, but its application in low-speed flow is still challenging, mainly due to limitations in the paint's pressure sensitivity and the camera performance. Model vibration and paint photodegradation can also cause significant errors, although the temperature problem is relatively insignificant due to the short duration of data acquisition and the possible use of a wind-on average as the reference image. Ideally, the resolution of instantaneous PSP data can be considered as the pressure change corresponding to 1 count variation out of the full count capacity of the camera, which is around 40 Pa for a 12-bit high-speed camera and a typical paint sensitivity of 0.7%/kPa. However, as Liu et al. (2001a) pointed out, the actual resolution is eventually limited by the photon shot noise of the camera, which was found to be over 900 Pa for a common high-speed camera (Peng et al. 2016c). Phase-averaging and spatial filtering are common methods for noise reduction, but their use limits spatial and temporal resolution. Thus, the main task here is to extract the clean pressure signal from a noisy background while preserving spatial and temporal resolution. A summary of noise-reduction methods is provided in Table 2, and will be elaborated in the following paragraphs.

Algorithms based on principal component analysis have shown great potential in noise reduction of time-resolved PSP data, and have effectively improved the detection limit of unsteady pressure. Advanced data-processing methods including single-value decomposition (SVD) and proper orthogonal decomposition (POD) can be directly applied to the PSP image sequence, generating a set of modes representing different features in the time-resolved data. If the SNR is sufficiently high, the main flow structures can be easily identified from those spatial features for further analysis. Unfortunately, for measurements in low-speed flows, which have low SNR, most of the modes are severely contaminated by noise. Therefore, the solution is to identify the modes closely related to the flow features and then perform reconstruction using those modes, as shown in Fig. 7. A basic method is to use the first N modes for reconstruction, as adopted by Gordeyev et al. (2014) for measurements on a turret at Ma = 0.33.

For applications at lower freestream speeds, the high level of noise demands more rigorous criteria for mode selection, which was achieved by scrutinizing the spatial contour and frequency spectrum of each mode (Pastuhoff et al. 2013; Peng et al. 2016c). Based on the comparison with referencing microphone data, this method allowed PSP to accurately resolve pressure fluctuation within 100 Pa with a freestream speed as low as 10 m/s. Nonetheless, the selection criteria of POD modes were non-ideal, as mainly based on subjective observation. Another issue was that the selected modes were still severely contaminated by noise, especially in cases with extremely low flow speeds, which would lead to a low-quality reconstruction. A solution for this, based on compressed data fusion, was recently proposed by Wen et al. (2018), which incorporated the clean data from scattered microphones to optimize the reconstruction of POD modes. This new method showed a 75% reduction in the reconstruction

Table 2 Noise reduction methods for unsteady PSP measurement in low-speed flows

| Noise reduction methods	Phase-averaging	Principal component analysis		Spectral analysis	
		POD/SVD	DMD	FFT band analysis	Coherent output power
Pressure fluctuation level	No	Yes	Yes	Yes	Yes
Periodic pressure history	Yes	Yes	Yes	No	No
Instantaneous pressure field	No	Yes	Yes	No	No
Applicability in flow with single/multiple dominant structures	Single	Single/multiple	Single/multiple	Single/multiple	Single/multiple
Reference	Yorita et al. (2010) Asai and Yorita (2011)	Pastuhoff et al. (2013) Gordeyev et al. (2014) Peng et al. (2016c) Wen et al. (2018)	Ali et al. (2016) Goßling et al. (2018)	Nakakita (2007) Asai and Yorita (2011)	Noda et al. (2018)
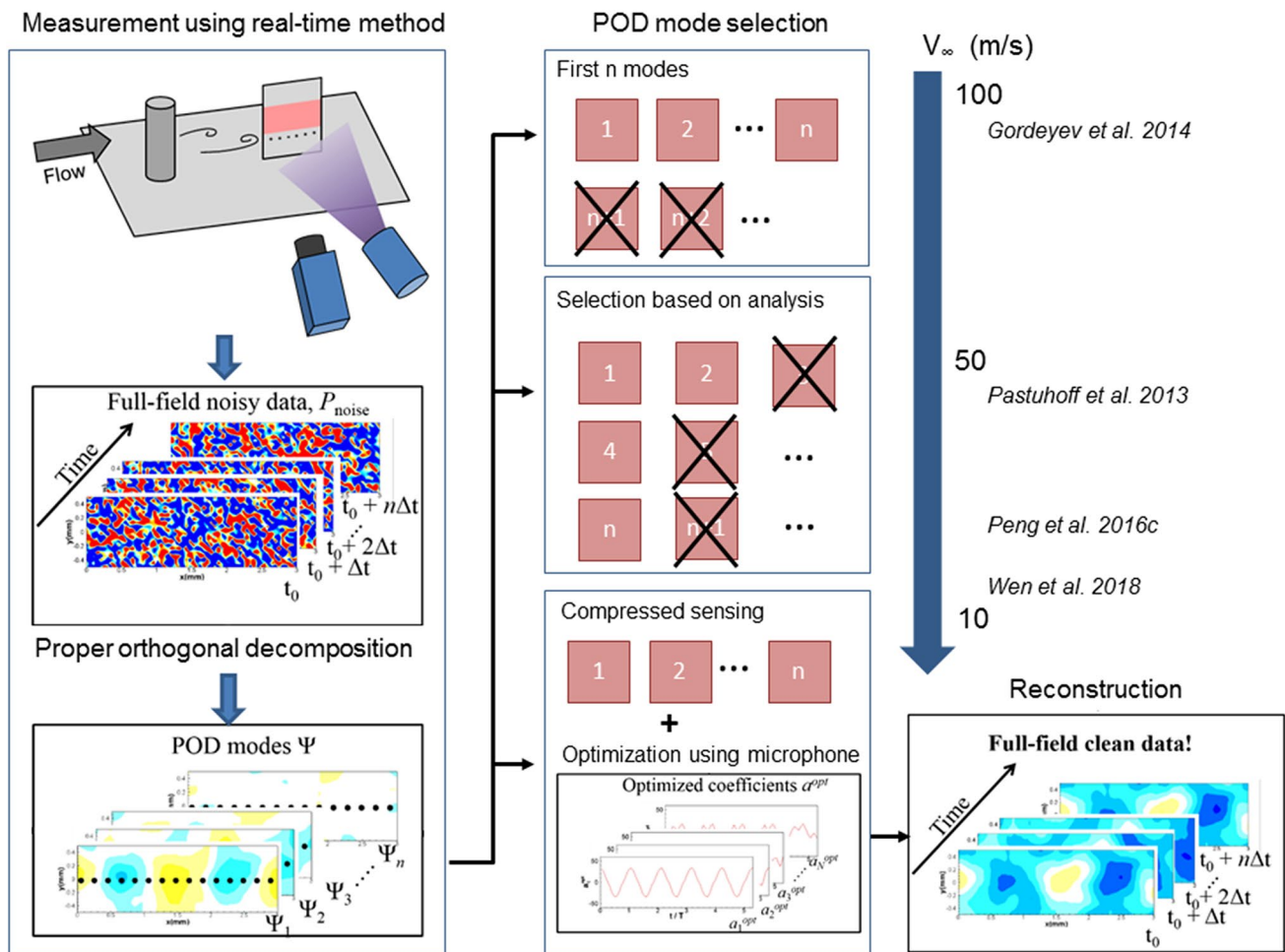
Fig. 7 Noise reduction methods based on proper orthogonal decomposition

error compared with previous POD analysis, and successfully recovered the unsteady pressure with amplitudes less than 50 Pa. In addition, dynamic mode decomposition (DMD) has also found applications in analyzing unsteady PSP data, which was less susceptible to noise contamination and more effective in extracting pressure features than POD (Ali et al. 2016; Goßling et al. 2018).

For a precise measurement of pressure fluctuation level in aeroacoustic applications, the frequency-domain method based on fast Fourier transform (FFT) is usually preferred. Nakakita (2011) compared the image-based method using a high-speed camera with the laser-scanning method using a PMT. The laser-scanning method had a lower noise level and better pressure resolution due to PMT's superior photosensitivity, while the image-based method had clear advantages in spatial resolution and time–cost. FFT band analysis is a common method to obtain the fluctuation level related to a certain spectral peak, achieved by summation over a certain frequency range (Nakakita 2007; Asai and Yorita 2011). Advanced techniques for spectral analysis were also

developed to extract other unsteady information in addition to the power spectrum, such as coherence, phase, and phase velocity (Nakakita 2013). More recently, a coherent output power (COP) method for power spectrum calculations was proposed by Noda et al. (2018), based on the cross-correlation between the PSP data and the signal from a pointwise sound-level meter. The COP method achieved a similar detection limit (~ 10 Pa^2) as the FFT method, and it was more effective in identification of the pressure fluctuation directly related to the noise source.

5.2 Hypersonic flow

Fast PSP has found applications in a variety of hypersonic tunnels with Mach number ranging from 5 to 10, as shown in Table 3. The major challenges of PSP measurement are summarized in Fig. 8 based on test duration and stagnation temperature. Implementation of fast PSP was initiated in shock tunnels, where the short test duration (< 100 ms) alleviated the temperature effect from aerodynamic heating

Table 3 List of fast PSP applications in hypersonic wind tunnels

References	PSP	TSP	Ma	t (s)	fps (Hz)	ΔT (K)	T correction
Hubner et al. (2001)	Thin-film		7.5	0.02	Single/4.5k	Small	In situ cal.
Nakakita et al. (2000)	AA	No	10	0.04	Single	< 2	In situ cal.
Sakaue et al. (2002b)	AA	No	4	0.2	Single	Small	In situ cal.
Kuriki et al. (2010); Morita et al. (2011)	AA	Yes	7	5–9	100/25	> 30	T-cancelled PSP
Yang et al. (2012)	AA	Yes	5	7.5	9	Unknown	In situ cal.
Peng et al. (2016b)	PC	Yes	5	3	500	10–70	TSP
Running et al. (2019)	AA	No	6	0.5	20k	< 3	IR

Fig. 8 Challenges of PSP measurement in hypersonic flow
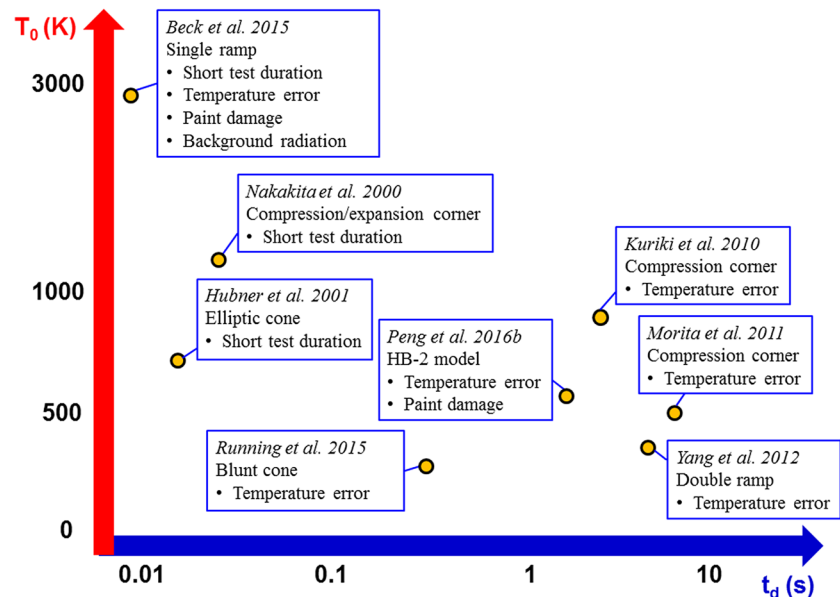
(Nakakita et al. 2000; Hubner et al. 2001; Sakaue et al. 2002b). An in situ calibration was generally sufficient to remove the temperature-induced error. As the application was extended to long-duration facilities with a run-time on the order of seconds, additional measures were required to counteract the strong temperature effects. A temperature-cancelled AA-PSP, which had an emission signal with low temperature-sensitivity within a specific spectral range was developed for this purpose, and was demonstrated in a high-enthalpy tunnel (Kuriki et al. 2010; Morita et al. 2011).

A different solution was to perform temperature correction using the temperature map measured by other means (TSP, infrared camera, etc.). Considering the general requirements for heat-flux measurement using TSP, a combined PSP/TSP measurement was appealing, as this could give complete flow-field information and enable temperature correction for PSP data. However, the conflicting requirements of the test model for PSP (highly heat-conductive model) and TSP (model with thermal insulation) measurements meant this was difficult to achieve (Watkins et al. 2009; Yang et al. 2012). Meanwhile, the PSP and TSP should have

overlapping excitation spectra, comparable intensity levels and similar thermal properties. Such a combined system was developed by Peng et al. (2016b) with a half-PSP/half-TSP configuration, and then applied to an HB-2 model to achieve simultaneous time-resolved measurement of pressure, temperature and heat flux in a Mach 5 flow. The accuracy of PSP measurement was significantly improved by use of a real-time temperature correction method using the TSP data. In a recent study, the temperature field on a blunt cone was obtained by infrared thermography, providing a correction for the unsteady pressure measured by AA-PSP (Running et al. 2019). PSP and infrared measurements were collected in separate runs due to interference between the two systems. The crossflow-induced boundary-layer separation was effectively identified by the full-field pressure fluctuations.

PSP measurements are facing additional challenges in the hostile environment of hypersonic flows, such as low SNR due to limited exposure time in shock tunnels and paint damage due to strong abrasion effect and flow contamination. For high-enthalpy facilities, another important issue is the background radiation due to the spontaneous emission of

high-enthalpy gas, which spectrally overlaps with the PSP signal and leads to large uncertainty (Beck et al. 2015). As the stagnation temperature and flow density increase, the strength radiation signal quickly grows and eventually overwhelms the PSP signal. This issue may be alleviated through optimized spectral filtering and camera gating, but it still limits the application of PSP in high-enthalpy flows.

5.3 Fast-rotating blades

Fast PSP measurements on rotating blades have three major challenges. First, short exposure time is necessary to freeze the motion, which leads to insufficient signal in each exposure and the need for a phase-averaging system to improve SNR. The phase-averaging method has found applications in various scenarios including turbocharger compressors (Gregory et al. 2002), helicopter rotors (Wong et al. 2005, 2010; Watkins et al. 2007) and rotating disks (Kameya et al. 2011), but it was unable to recognize high-frequency pressure features and cycle-to-cycle variations. As discussed in Sect. 2, a single-shot lifetime-based technique was developed to solve this problem (Gregory et al. 2009; Juliano et al.

2011). The second challenge is the image blur when using the phase-averaging method, caused by the finite exposure time and cycle-to-cycle variations in blade position. This can be partially resolved by the single-shot method, but image blur is still pronounced at high rotation, due to the finite luminescent lifetime of PSP (usually a few μs). A further solution is to recover clear images from the blurred images via a deconvolution-based deblurring algorithm (Juliano et al. 2012; Gregory et al. 2014b). The third challenge is the inherent temperature-induced error in PSP measurement, which usually results from an aerodynamic heating-driven radial temperature gradient on the blade surface. Typically, temperature corrections in this context are based on the temperature fields obtained from separate measurements using TSP (Juliano et al. 2012; Klein et al. 2013) or infrared thermography (Pastuhoff et al. 2016).

As shown in Fig. 9, the single-shot lifetime technique with image-deblurring and temperature-correction capabilities (using TSP) is arguably the most effective method for fast PSP measurement on fast-rotating blades, and has been successfully utilized in helicopter rotor wind-tunnel tests on small to large scales (Wong et al. 2012; Disotell
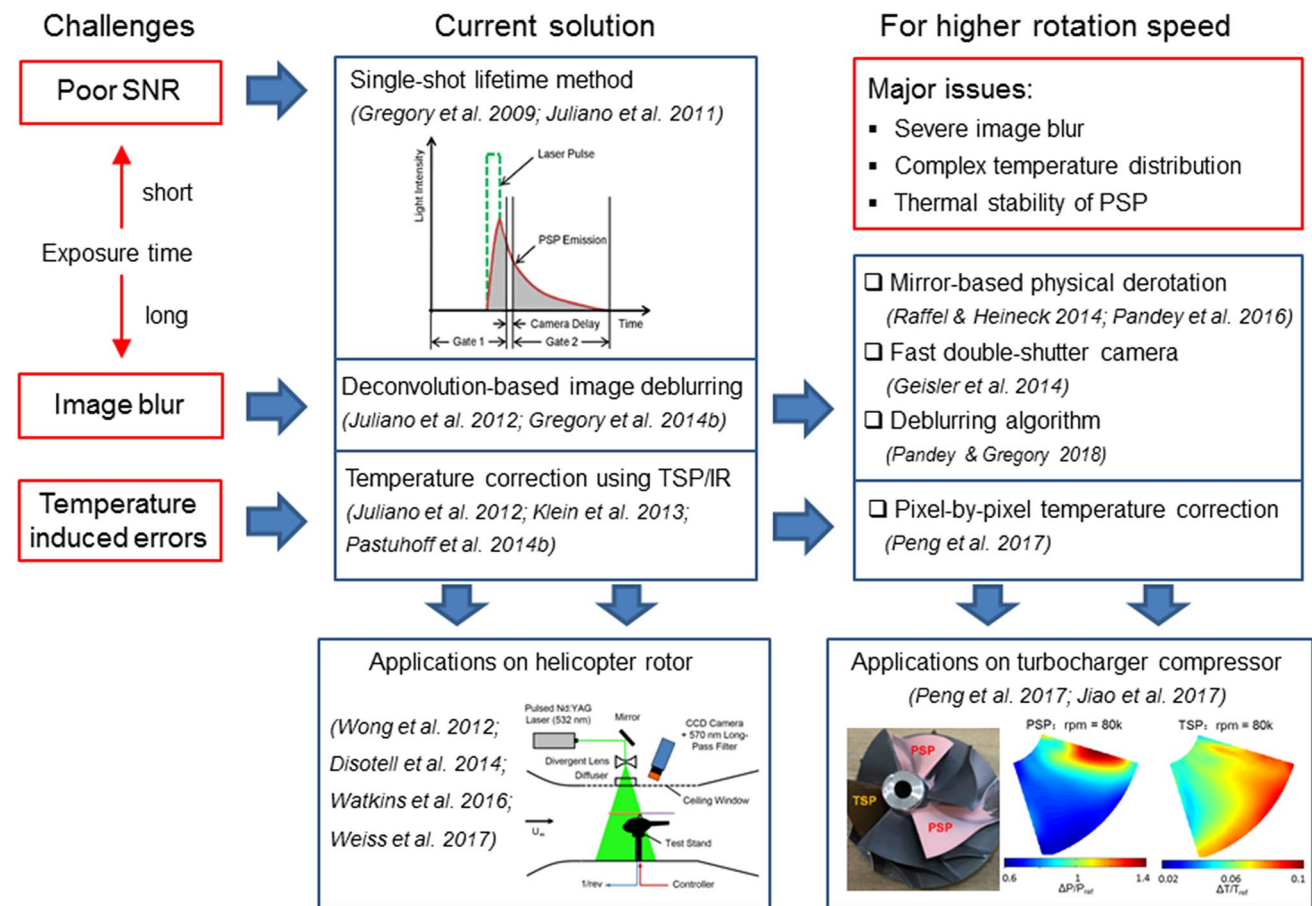

Fig. 9 Challenges and recent advances of PSP measurement on fast-rotating blades

et al. 2014; Watkins et al. 2016). Despite its limited sampling rate, this method was able to identify unsteady flow features from the cycle-to-cycle variations in transient pressure data (Disotell et al. 2014, 2016). Recent efforts have focused on improving its measurement accuracy via developments in both its hardware and its data-processing algorithm.

As shown by Gregory et al. (2014b), the deconvolution-based image-deblurring method has the following limitations: (1) performance-degradation for images with low SNR, due to the amplification of random noise; (2) high-frequency ringing-noise near edges of the PSP sample, due to the Gibbs effect; and (3) errors in areas with large pressure gradients, due to the use of a constant lifetime for deblurring. Therefore, further reduction or even elimination of image blur is still desirable. A physical mirror-based derotation method was proposed for image-blur prevention, but the installment and alignment of such an optical system would be challenging for large-scale wind tunnel tests (Raffel and Heineck 2014; Pandey et al. 2016). A more practical solution was the development of a fast double-shutter CCD camera with a controllable exposure of G2 (Geisler 2014), which was shown to greatly reduce the amount of blur in the original long exposure. This updated single-shot system effectively minimized the errors related to image-blur during PSP measurement on helicopter rotor blades (Weiss et al. 2017). More recently, an improved image-deblurring algorithm was developed by introducing an iterative scheme that allowed incorporation of spatially variant lifetimes (Pandey and Gregory 2018), demonstrating superior performance in recovery of sharp intensity/pressure changes.

The advances in measurement technique have made PSP measurement possible on fast-rotating blades in turbomachinery. A representative work was the simultaneous PSP and TSP measurements conducted by Jiao et al. (2017) on turbocharger compressor blades with a maximum tip speed of over 300 m/s. The high rotation speed not only posed challenges for paint robustness, it also led to low signal level, severe image-blur and a strong temperature gradient. In particular, both streamwise and radial temperature gradients were present on the blade at high rotation speed, as shown in the bottom right of Fig. 9. Accordingly, this complex temperature distribution necessitated high-quality TSP results and a pixel-by-pixel temperature-correction scheme for processing PSP data (Peng et al. 2017). It should be noted that a bottleneck problem was the questionable thermal stability of PSP at higher temperatures (> 350 K), which would be regularly encountered in turbomachinery testing facilities. The potential solution regarding this issue will be discussed in the following section.

5.4 Towards high-temperature environment

Due to the moderate operating temperature of conventional wind tunnels, the performance of PSP at elevated temperatures has thus far received little attention. However, now that PSP is being used in harsher environments (hypersonic tunnels, turbomachines, etc.), the possibility of its potential thermal degradation or even complete failure has become a major concern. Intensity degradation was originally observed in pyrene-based PSP at temperatures higher than 323 K (Mebarki 1998), which was attributed to diffusion and evaporation of pyrene. It could be mitigated by restricting the diffusion process with a strong binder (Basu et al. 2003, 2009). Gouin and Gouterman (2000) studied the effect of heat treatment on FIB-based PSP, finding that an annealing temperature of 423 K would cause destructive effects to PSP's sensing properties. With respect to fast PSP, recent results showed irreversible changes in the lifetime of PC-PSP following a 30-min heat treatment at 333 K or above (Peng et al. 2019a), with temperatures > 373 K causing severe nonlinearity in the calibration curve. The findings are consistent with the recommended operating temperature range (273–353 K) listed for a commercially available porous PSP (FP-PSP from Innovative Scientific Solution Inc.). Although the mechanism of this thermal degradation effect is yet to be explored, the failure of PSP in high-temperature environments may be inevitable, considering the typically limited thermal stability of organic compounds.

Encouragingly, the recent discovery of a so-called "oxygen quenching" mechanism in thermographic phosphors suggests that it may be possible to develop high-temperature PSP based on inorganic materials. A few early studies reported the effect of oxygen on the luminescent property of europium-doped phosphors including Y_2O_3:Eu and Eu-doped yttria stabilized zirconia (YSZ:Eu) (Feist et al. 2003; Brubach et al. 2007; Shen and Clarke 2009). However, it was only recently that a systematic study was conducted by Yang et al. (2018) to determine the underlying mechanism. Above its quenching temperature (400–700 K, depending on the phosphor), the lifetime and intensity of the phosphor decreased as the oxygen concentration increased. This "oxygen quenching" phenomenon was attributed to the existence of oxygen vacancies in the host lattice, and distinct from the mechanism of direct interaction between oxygen and excited luminophore in regular, organic compound-based PSPs. Subsequent work showed that there were pronounced pressure sensitivities in Y_2O_3:Eu at temperatures over 800 K (see Fig. 10), indicating that the "oxygen quenching" effect in phosphors could be used for pressure measurement at high temperatures. Nonetheless, a substantial amount of work is still required to fully establish the theoretical basis of this effect, and identify phosphors with sufficiently high pressure sensitivity within certain, desirable temperature ranges.
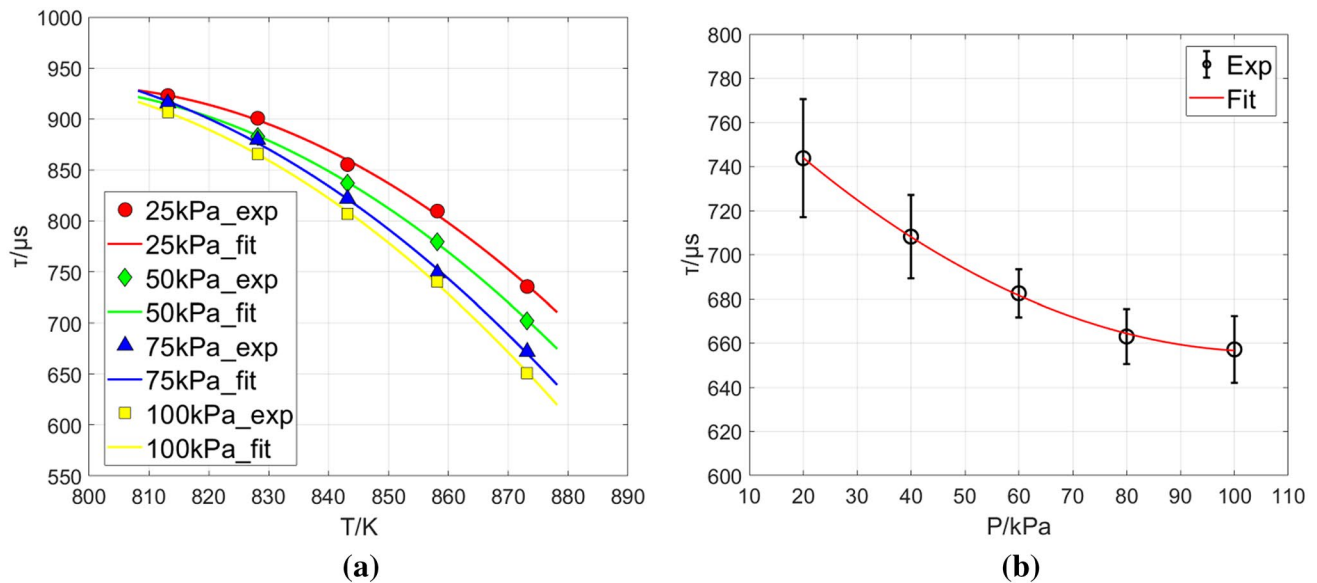
Fig. 10 Pressure sensing property of phosphor Y_2O_3:Eu: **a** temperature calibration curves at different pressure values, **b** pressure calibration curve at 873 K

6 Conclusion and outlook

The application of fast PSP has greatly expanded over the past two decades, thanks to phenomenal advances in porous paint development and measurement strategies. While the technology has mostly matured for real-time unsteady measurement in conventional wind tunnels, recent efforts are focused on resolving smaller pressure fluctuations in a wider range of test environments.

The key points of this review are given below:

1. The response time of newly developed fast PSPs has reached the order of 10 μs or less, which is similar to the luminophore's lifetime. The effects of oxygen diffusion and luminescent lifetime are equally important in the modeling of fast PSP's dynamic response. Other factors such as paint thickness, luminophore distribution and light attenuation should also be considered.
2. Advanced manufacturing technology has enabled breakthroughs in PSP's sensing property and innovations in multi-functional coatings. Novel integrated PSP system concepts have provided solutions for key problems in optical arrangement.
3. Fast PSP exhibits superior performance than conventional PSP in low-speed applications. Noise-reduction techniques have greatly enhanced its capability to resolve small pressure fluctuations, but there is still a trade-off versus spatial/temporal resolution and the pressure detection limit, due to limitations in imaging hardware.

4. PSP has emerged as a valuable technique for study of hypersonic flow and fast-rotating blades, and the development of pressure-sensitive phosphors suggests that it may also find application in high-temperature environments. The temperature effect is the main source of error in these challenging environments, necessitating high-accuracy corrections utilizing elaborate temperature measurement.

In the foreseeable future, the expansion and enhancement of PSP technology will require more multidisciplinary research. Some important issues are identified below along with proposed solutions.

1. Paint development: as its response time already reached the 1-μs mark, the performance of fast PSP is now limited by other factors such as insufficient signal strength and pressure sensitivity. Comprehensive study should be made concerning the photophysical mechanism of luminescence and the molecular interaction between luminophore and binder materials. A deeper understanding of these processes will facilitate breakthroughs in sensing properties, via micro- and nanoscale manipulations of the energy-transfer process underpinning luminescence.
2. Measurement system: Highly integrated and intelligent PSP systems are expected to accommodate the diverse requirements of a wide range of test environments. The frontier technology of robotics and machine vision may help shape the next-generation PSP systems, as seen in the recent development of automatic particle image velocimetry (PIV) systems (Michaux et al. 2018). The

merging of PSP with other techniques (TSP, DIC, etc.) is also desirable, as this will enable multi-field measurement for the study of complex flow problems.

3. Data processing and analysis: Noise-reduction methods must keep evolving to further extend the detection limit of fast PSP, and an equally pressing task is to best use the rich data set generated by this technique for turbulence research. To this end, the data assimilation technique (Law et al. 2015) has emerged as a promising tool for integrating PSP measurement and CFD simulation to eventually achieve the high-fidelity prediction of turbulent flows.

References

Ali MY, Pandey A, Gregory JW (2016) Dynamic mode decomposition of fast pressure sensitive paint data. Sensors. https://doi.org/10.3390/s16060862

Asai K, Yorita D (2011) Unsteady PSP measurement in low-speed flow—overview of recent advancement at Tohoku University. In: 49th AIAA aerospace sciences meeting including the new horizons forum and aerospace exposition, AIAA 2011-847

Basu BJ, Anandan C, Rajam KS (2003) Study of the mechanism of degradation of pyrene-based pressure sensitive paints. Sens Actuators B Chem 94:257–266

Basu BJ, Vasantharajan N, Raju C (2009) A novel pyrene-based binary pressure sensitive paint with low temperature coefficient and improved stability. Sens Actuators B-Chem 138:283–288

Beck WH, Klein C, Henne U, Sachs W, Schramm JM, Wagner A, Hannemann K, Gawehn T, Gülhan A (2015) Application of temperature and pressure sensitive paints to DLR hypersonic facilities: "lessons learned". In: 53rd AIAA aerospace sciences meeting, AIAA-2015-0023

Bell JH (2001) Accuracy limitations of lifetime-based pressure-sensitive paint (PSP) measurements. In: 19th international congress on instrumentation in aerospace simulation facilities, https://doi.org/10.1109/iciasf.2001.960231

Bitter M, Hara T, Hain R, Yorita D, Asai K, Kahler CJ (2012) Characterization of pressure dynamics in an axisymmetric separating/reattaching flow using fast-responding pressure-sensitive paint. Exp Fluids 53:1737–1749. https://doi.org/10.1007/s00348-012-1380-7

Brubach J, Dreizler A, Janicka J (2007) Gas compositional and pressure effects on thermographic phosphor thermometry. Meas Sci Technol 18:764–770. https://doi.org/10.1088/0957-0233/18/3/028

Chin D, Sealy W, Granlund K, Hayashi T, Sakaue H (2017) Unsteady PSP measurements on a cylinder translating out from a supersonic cavity. In: 47th AIAA fluid dynamics conference, AIAA-2017-3468

Claucherty S, Sakaue H (2019) Pyrene based polymer ceramic pressure-sensitive paint for aerodynamic application. In: AIAA Scitech 2019 Forum, AIAA-2019-0020

Crafton J, Fonov S, Forlines R, Palluconi S (2013) Development of pressure-sensitive paint systems for low speed flows and large wind tunnels. In: 51st AIAA aerospace sciences meeting, AIAA 2013-0482. https://doi.org/10.2514/6.2013-482

Crafton J, Forlines A, Palluconi S, Hsu K, Carter C, Gruber M (2015) Investigation of transverse jet injections in a supersonic crossflow using fast-responding pressure-sensitive paint. Exp Fluids 56:27. https://doi.org/10.1007/s00348-014-1877-3

Davis T, Edstrand A, Alvi F, Cattafesta L, Yorita D, Asai K (2015) Investigation of impinging jet resonant modes using unsteady pressure-sensitive paint measurements. Exp Fluids 56:101. https://doi.org/10.1007/s00348-015-1976-9

Dickey EC, Varghese OK, Ong KG, Gong D, Paulose M, Grimes CA (2002) Room temperature ammonia and humidity sensing using highly ordered nanoporous alumina films. Sensors 2:91–110. https://doi.org/10.3390/s20300091

Disotell KJ, Peng D, Juliano TJ, Gregory JW, Crafton JW, Komerath NM (2014) Single-shot temperature- and pressure-sensitive paint measurements on an unsteady helicopter blade. Exp Fluids 55:1671. https://doi.org/10.1007/s00348-014-1671-2

Disotell KJ, Nikoueeyan P, Naughton JW, Gregory JW (2016) Global surface pressure measurements of static and dynamic stall on a wind turbine airfoil at low Reynolds number. Exp Fluids 57:82. https://doi.org/10.1007/s00348-016-2175-z

Egami Y, Fujii K, Takagi T, Matsuda Y, Yamaguchi H, Niimi T (2013) Reduction of temperature effects in pressure-sensitive paint measurements. AIAA J 51:1779–1782. https://doi.org/10.2514/1.J052226

Egami Y, Ueyama J, Furukawa S, Kameya T, Matsuda Y, Yamaguchi H, Niimi T (2015) Development of fast response bi-luminophore pressure-sensitive paint by means of an inkjet printing technique. Meas Sci Technol 26(064004):1–8. https://doi.org/10.1088/0957-0233/26/6/064004

Egami Y, Konishi S, Sato Y, Matsuda Y (2019a) Effects of solvents for luminophore on dynamic and static characteristics of sprayable polymer/ceramic pressure-sensitive paint. Sens Actuators A-Phys 286:188–194. https://doi.org/10.1016/j.sna.2018.12.034

Egami Y, Sato Y, Konihsi S (2019b) Development of sprayable pressure sensitive paint with a response time of less than 10 μs. AIAA J 57:2198–2203. https://doi.org/10.2514/1.J057434

Fang S, Long SR, Disotell KJ, Gregory JW, Semmelmayer FC, Guyton RW (2012) Comparison of unsteady pressure-sensitive paint measurement techniques. AIAA J 50:209–222. https://doi.org/10.2514/1.J051167

Feist JP, Heyes AL, Seedfeldt S (2003) Oxygen quenching of phosphorescence from thermographic phosphors. Meas Sci Technol 14:17

Fischer LH, Karakus C, Meier RJ, Risch N, Wolfbeis OS, Holder E, Schaferling M (2012) Referenced dual pressure- and temperature-sensitive paint for digital color camera read out. Chem Eur J 18:15706–15713. https://doi.org/10.1002/chem.201201358

Flaherty W, Reedy TM, Elliott GS, Austin JM, Schmit RF, Crafton J (2014) Investigation of cavity flow using fast-response pressure-sensitive paint. AIAA J 52:2462–2470. https://doi.org/10.2514/1.J052864

Fujii S, Numata D, Nagai H, Asai K (2013) Development of ultrafast-response anodized-aluminum pressure-sensitive paints. AIAA 2013-0485

Gardner AD, Klein C, Sachs WE, Henne U, Mai H, Richter K (2014) Investigation of three-dimensional dynamic stall on an airfoil using fast-response pressure-sensitive paint. Exp Fluids 55:1807. https://doi.org/10.1007/s00348-014-1807-4

Geisler R (2014) A fast double shutter system for CCD image sensors. Meas Sci Technol 25:025404. https://doi.org/10.1088/0957-0233/25/2/025404

Gordeyev S, De Lucca N, Jumper EJ, Hird K, Juliano TJ, Gregory JW, Thordahl J, Wittich DJ (2014) Comparison of unsteady pressure fields on turrets with different surface features using

pressure-sensitive paint. Exp Fluids 55(1661):1–20. https://doi.org/10.1007/s00348-013-1661-9

Goss L, Trump D, Sarka B, Lydick L, Baker W (2000) Multi-dimensional time-resolved pressure-sensitive paint techniques: a numerical and experimental comparison. In: 37th AIAA aerospace sciences meeting and exhibit, AIAA-2000-0832. https://doi.org/10.2514/6.2000-832

Goßling J, Ahlefeldt T, Mumcu A, Hilfer M (2018) Experimental validation of unsteady pressure-sensitive paint for acoustic applications. In: 5th international conference on experimental fluid mechanics

Gouin S, Gouterman M (2000) Ideality of pressure-sensitive paint II. Effect of annealing on the temperature dependence of the luminescence. J Appl Polym Sci 77:2805–2814

Gregory JW, Sullivan JP (2006) Effect of quenching kinetics on unsteady response of pressure-sensitive paint. AIAA J 44:634–645

Gregory JW, Sakaue H, Sullivan JP (2002) Unsteady Pressure measurements in a turbocharger compressor using porous pressure-sensitive paint. In: Proceedings of the 40th AIAA aerospace sciences meeting and exhibit, AIAA 2002-0084

Gregory JW, Sullivan JP, Wanis S, Komerath NM (2006) Pressure-sensitive paint as a distributed optical microphone array. J Acoust Soc Am 119:251–261

Gregory JW, Sullivan JP, Raman G, Raghu S (2007) Characterization of the microfluidic oscillator. AIAA J 45:568–576

Gregory JW, Asai K, Kameda M, Liu T, Sullivan JP (2008) A review of pressure-sensitive paint for high-speed and unsteady aerodynamics. P I Mech Eng G-J Aer 222:249–290. https://doi.org/10.1243/09544100JAERO243

Gregory JW, Kumar P, Peng D, Fonov S, Crafton J, Liu T (2009) Integrated optical measurement techniques for investigations of fluid-structure interactions. In: 39th AIAA Fluid dynamics conference, AIAA 2009-4044

Gregory JW, Sakaue H, Liu T, Sullivan JP (2014a) Fast pressure-sensitive paint for flow and acoustic diagnostics. Ann Rev Fluid Mech 56:303–330. https://doi.org/10.1146/annurev-fluid-010313-141304

Gregory JW, Disotell KJ, Peng D, Juliano TJ, Crafton J, Komerath NM (2014b) Inverse methods for deblurring pressure-sensitive paint images of rotating surfaces. AIAA J 52:2045–2061

Hayashi T, Sakaue H (2017) Dynamic and steady characteristics of polymer-ceramic pressure-sensitive paint with variation in layer thickness. Sensors 17(1125):1–9. https://doi.org/10.3390/s17051125

Hayashi T, Houpt A, Hedlund B, Leonov S, Sakaue H (2018) Two-color polymer-ceramic pressure-sensitive paint for transient plasma in M = 2 Airflow. In: 2018 AIAA aerospace sciences meeting, AIAA-2018-1028

Holmes JW (1998) Analysis of radiometric, lifetime and fluorescent lifetime imaging for pressure sensitive paint. Aeronaut J 102:189

Hubner JP, Carroll BF, Schanze KS, Ji HF, Holden MS (2001) Temperature- and pressure-sensitive paint measurements in short-duration hypersonic flow. AIAA J 39:654–659. https://doi.org/10.2514/2.1358

Hyakutake T, Taguchi H, Kato J, Nishide H, Watanabe M (2009) Luminescent multi-layered polymer coating for the simultaneous detection of oxygen pressure and temperature. Macromol Chem Phys 210:1230–1234. https://doi.org/10.1002/macp.200900176

Iijima Y, Sakaue H (2011) Development of electroluminescence based pressure-sensitive paint system. Rev Sci Instr 82:015107. https://doi.org/10.1063/1.3514987

Ishii M, Isokawa H, Miyazaki T, Sakaue H (2017a) Surface state measurement of a free-flight object by motion-capturing method. In: 55th AIAA aerospace sciences meeting, AIAA-2017-0943

Ishii M, Miyazaki T, Sakaue H (2017b) Uniformity study of two-functional luminescent dyes adsorbed over an anodized aluminum coating for motion-capturing pressure- and temperature-sensitive paint imaging. Sensors 18:26. https://doi.org/10.3390/s18010026

Jiao L, Peng D, Yu Y, Liu Y, Oshio T, Oouchida S, Kawakubo T, Yakushiji A (2017) Single-shot lifetime-based PSP and TSP measurements on rotating blades—challenges at high RPMs. In: 33rd AIAA aerodynamic measurement technology and ground testing conference, AIAA-2017-3735

Jiao L, Chen Y, Peng D, Liu Y, Gregory JW (2018a) Experimental study of the interaction between rotor wake and a cylinder in Hover. In: 2018 applied aerodynamics conference, AIAA-2018-4214

Jiao L, Peng D, Liu Y (2018b) Dynamic response of polymer ceramic pressure-sensitive paint: improved model considering thickness effect. AIAA J 56:2903–2906. https://doi.org/10.2514/1.J056778

Juliano TJ, Kumar P, Peng D, Gregory JW, Crafton J, Fonov S (2011) Single-shot, lifetime-based pressure-sensitive paint for rotating blades. Meas Sci Tech 22:085403. https://doi.org/10.1088/0957-0233/22/8/085403

Juliano TJ, Disotell KJ, Gregory JW, Crafton JW, Fonov SD (2012) Motion-deblurred, fast-response pressure-sensitive paint on a rotor in forward flight. Meas Sci Tech 23:045303. https://doi.org/10.1088/0957-0233/23/4/045303

Kameda M (2012) Effect of luminescence lifetime on the frequency response of fast-response pressure-sensitive paints. Trans Jpn Soc Mech Eng Ser B 78:1942–1950. https://doi.org/10.1299/kikaib.78.1942

Kameda M, Tezuka N, Hangai T, Asai K, Nakakita K, Amao Y (2004) Adsorptive pressure-sensitive coatings on porous anodized aluminium. Meas Sci Technol 15:489–500

Kameda M, Tabei T, Nakakita K, Sakaue H, Asai K (2005) Image measurements of unsteady pressure fluctuation by a pressure-sensitive coating on porous anodized aluminium. Meas Sci Technol 16:2517–2524. https://doi.org/10.1088/0957-0233/16/12/017

Kameda M, Seki H, Makoshi T, Amao Y, Nakakita K (2012) A fast-response pressure sensor based on a dye-adsorbed silica nanoparticle film. Sensor Actuat B-Chem 171:343–349

Kameda M, Yoshida M, Sekiya T, Nakakita K (2015) Humidity effects in the response of a porous pressure-sensitive paint. Sens Actuators B Chem 208:399–405. https://doi.org/10.1016/j.snb.2014.11.052

Kameya T, Matsuda Y, Yamaguchi H, Egami Y, Niimi T (2011) Pressure-sensitive paint measurement on co-rotating disks in a hard disk drive. Opt Laser Eng 10:1016

Kameya T, Matsuda Y, Egami Y, Yamaguchi H, Niimi T (2014) Dual luminescent arrays sensor fabricated by inkjet-printing of pressure- and temperature-sensitive paints. Sens Actuators B Chem 190:70–77. https://doi.org/10.1016/j.snb.2013.08.011

Kautsky H, Hirsch H (1935) Detection of minutest amounts of oxygen by extinction of phosphorescence (in German). Z Anorg Allg Chem 222:126

Klein C, Henne U, Sachs WE, Engler RH, Egami Y, Ondrus V, Beifuss U, Mai H (2007) Application of pressure-sensitive paint for determination of dynamic surface pressures on a rotating 65° delta wing and an oscillating 2D profile in transonic flow. In: 2007 22nd international congress on instrumentation in aerospace simulation facilities, ICIASF, Art. No.: 4380887; CODEN: ICREE. https://doi.org/10.1109/iciasf.2007.4380887

Klein C, Henne U, Sachs W, Hock S, Falk N, Beifuss U, Ondrus V, Schaber S (2013) Pressure measurement on rotating propeller blades by means of the pressure-sensitive paint lifetime method. In: 51st AIAA aerospace sciences meeting, AIAA-2013-0483

Kuriki T, Sakaue H, Imamura O, Suzuki K (2010) Temperature-cancelled AA-PSP for hypersonic compression corner flows.

In: 48th AIAA aerospace sciences meeting including the new horizons forum and aerospace exposition, AIAA 2010-673

Law KJ, Stuart AM, Zygalakis KC (2015) Data assimilation: a mathematical introduction. e-print arXiv:1506.07825

Li R, Gao L, Zheng T, Yang G (2018) Experimental investigation on static/dynamic characteristics of a fast-response pressure sensitive paint. Chin J Aeronaut 31:1198–1205. https://doi.org/10.1016/j.cja.2018.04.006

Liu T, Sullivan JP (2005) Pressure and temperature sensitive paints. Springer, New York

Liu T, Campbell BT, Burns SP, Sullivan JP (1997) Temperature- and pressure-sensitive luminescent paints in aerodynamics. Appl Mech Rev 50:227–246

Liu T, Guille M, Sullivan JP (2001a) Accuracy of pressure-sensitive paint. AIAA J 39:103–112

Liu T, Teduka N, Kameda M, Asai K (2001b) Diffusion timescale of porous pressure-sensitive paint. AIAA J 39:2400–2402. https://doi.org/10.2514/2.1249

Lo KH, Kontis K (2016) Static and wind-on performance of polymer-based pressure-sensitive paints using platinum and ruthenium as the luminophore. Sensors 16(595):1–17. https://doi.org/10.3390/s16050595

Mao Y, Gao Y, Wu S, Wu S, Shi J, Zhou B, Tian Y (2017) Highly enhanced sensitivity of optical oxygen sensors using microstructured PtTFPP/PDMS-pillar arrays sensing layer. Sens Actuators B-Chem 251:495–502. https://doi.org/10.1016/j.snb.2017.05.081

Matsuda H, Fukuda K (1995) Ordered metal nanohole arrays made by a two-step replication of honeycomb structures of anodic alumina. Science 268:1466–1468

Matsuda Y, Uchida T, Suzuki S, Misaki R, Yamaguchi H, Niimi T (2011) Pressure-sensitive molecular film for investigation of micro gas flows. Micorfluid Nanofluid 10:165–171. https://doi.org/10.1007/s10404-010-0664-6

Matsuda Y, Ueno K, Yamaguchi H, Egami Y, Niimi T (2012) Organic electroluminescent sensor for pressure measurement. Sensors 12:13899–13906. https://doi.org/10.3390/s121013899

Matsuda Y, Yorita D, Egami Y, Kameya T, Kakihara N, Yamaguchi H, Asai K, Niimi T (2013) Unsteady pressure-sensitive paint measurement based on the heterodyne method using low frame rate camera. Rev Sci Instr 84(105110):1–5. https://doi.org/10.1063/1.4826085

Matsuda Y, Uchida K, Egami Y, Yamaguchi H, Niimi T (2016) Polymer-particle pressure-sensitive paint with high photostability. Sensors 16(550):1–7. https://doi.org/10.3390/s16040550

Matsuda Y, Kameya T, Suzuki Y, Yoshida Y, Egami Y, Yamaguchi H, Niimi T (2017) Fine printing of pressure- and temperature-sensitive paints using commercial inkjet printer. Sens Actuators BChem 250:563–568. https://doi.org/10.1016/j.snb.2017.04.188

McGraw CM, Bell JH, Khalil G, Callis JB (2006) Dynamic surface pressure measurements on a square cylinder with pressure sensitive paint. Exp Fluids 40:203–211

McMullen RM, Huynh DP, Gregory JW, Crafton J (2013) Dynamic calibrations for fast-response porous polymer/ceramic pressure-sensitive paint. In: AIAA ground testing conference, AIAA 2013-3123

Mebarki Y (1998) Pressure sensitive paints: application in wind tunnels. ONERA NT 1998-6

Merienne MC, Coponet D, Luyssen JM (2012) Transient pressure-sensitive-paint investigation in a nozzle. AIAA J 50:1453–1461. https://doi.org/10.2514/1.J050926

Merienne MC, Le Sant Y, Lebrun F, Deleglise B, Sonnet D (2013) Transonic buffeting investigation using unsteady pressure-sensitive-paint in a large wind tunnel. In: 51st AIAA aerospace sciences meeting, AIAA-2013-1136

Merienne MC, Molton P, Bur R, Le Sant Y (2015) Pressure-sensitive paint application to an oscillating shock wave in a transonic flow. AIAA J 53:3208–3220. https://doi.org/10.2514/1.J053744

Michaux F, Mattern P, Kallweit S (2018) RoboPIV: how robotics enable PIV on a large industrial scale. Meas Sci Technol 29:074009. https://doi.org/10.1088/1361-6501/aab5c1

Moon K, Mori H, Ambe Y, Kawabata H (2012) Development of dual-layer PSP/TSP system for pressure and temperature measurement in low-speed flow field. In: Proceedings of the ASME-JSME-KSME 2011 joint fluids engineering conference, AJK 2011-11020

Moon K, Mori H, Furukawa M (2018) Simultaneous measurement method of pressure and temperature using dual-layer PSP/TSP with lifetime-based method. Meas Sci Technol 29:125301. https://doi.org/10.1088/1361-6501/aae408

Morita K, Suzuki K, Imamura O, Sakaue H (2011) Temperature-cancelled anodized-aluminum pressure sensitive paint for hypersonic wind tunnel application. In: 41st AIAA fluid dynamics conference and exhibit, AIAA-2011-3724

Nakakita K (2007) Unsteady pressure distribution measurement around 2D-cylinders using pressure-sensitive paint. In: 25th AIAA applied aerodynamics conference, AIAA 2007-3819. https://doi.org/10.2514/6.2007-3819

Nakakita K (2011) Unsteady pressure measurement on NACA0012 model using global low-speed unsteady PSP technique. In: 41st AIAA fluid dynamics conference and exhibit, AIAA 2011-3901

Nakakita K (2013) Detection of phase and coherence of unsteady pressure field using unsteady PSP measurement. In: AIAA ground testing conference, AIAA-2013-3124

Nakakita K, Yamazaki T, Asai K, Teduka N, Fuji A, Kameda M (2000) Pressure sensitive paint measurement in a hypersonic shock tunnel. In: 21st AIAA aerodynamic measurement technology and ground testing conference, AIAA 2000-2523. https://doi.org/10.2514/6.2000-2523

Nakakita K, Takama Y, Imagawa K, Kato H (2012) Unsteady PSP measurement of transonic unsteady flow field around a rocket fairing model. In: 28th aerodynamic measurement technology, ground testing, and flight testing conference, AIAA-2012-2758

Noda T, Nakakita K, Wakahara M, Kameda M (2018) Detection of small-amplitude periodic surface pressure fluctuation by pressure-sensitive paint measurements using frequency-domain methods. Exp Fluids. https://doi.org/10.1007/s00348-018-2550-z

Ogg DR, Rice BE, Peltier SJ, Staines JT, Claucherty SL, Combs CS (2018) Simultaneous stereo digital image correlation and pressure-sensitive paint measurements of a compliant panel in a Mach 2 wind tunnel. In: 2018 fluid dynamics conference, AIAA-2018-3869

Panda J (2017) Experimental verification of buffet calculation procedure using unsteady pressure-sensitive paint. J Aircraft 54:1791–1801. https://doi.org/10.2514/1.C033917

Pandey A, Gregory JW (2015) Step response characteristics of polymer/ceramic pressure-sensitive paint. Sensors 15:22304–22324. https://doi.org/10.3390/s150922304

Pandey A, Gregory JW (2016) Frequency-response characteristics of polymer/ceramic pressure-sensitive paint. AIAA J 54:174–185. https://doi.org/10.2514/1.J054166

Pandey A, Gregory JW (2018) Iterative blind deconvolution algorithm for deblurring a single PSP/TSP image of rotating surfaces. Sensors 18:3075. https://doi.org/10.3390/s18093075

Pandey A, Gregory JW, Stansfield S, Crafton J (2016) Comparison of blur elimination techniques for PSP images of rotating surfaces. In: 54th AIAA aerospace sciences meeting, AIAA-2016-2019

Pastuhoff M, Yorita D, Asai K, Alfredsson PH (2013) Enhancing the signal-to-noise ratio of pressure sensitive paint data by singular value decomposition. Meas Sci Technol 24:075301. https://doi.org/10.1088/0957-0233/24/7/075301

Pastuhoff M, Tillmark N, Alfredsson PH (2016) Measuring surface pressure on rotating compressor blades using pressure sensitive paint. Sensors 16:344. https://doi.org/10.3390/s16030344

Peng D, Liu Y (2016) A grid-pattern PSP/TSP system for simultaneous pressure and temperature measurements. Sens Actuators B Chem 222:141–150. https://doi.org/10.1016/j.snb.2015.08.070

Peng D, Jensen CD, Juliano TJ, Gregory JW, Crafton J, Palluconi S, Liu T (2013) Temperature-compensated fast pressure-sensitive paint. AIAA J 51:2420–2431. https://doi.org/10.2514/1.J052318

Peng D, Jiao L, Liu Y (2016a) Development of a grid PSP/TSP system for unsteady measurements on rotating surfaces. In: 32nd AIAA aerodynamic measurement technology and ground testing conference, AIAA 2016-3405

Peng D, Jiao L, Sun Z, Gu Y, Liu Y (2016b) Simultaneous PSP and TSP measurements of transient flow in a long-duration hypersonic tunnel. Exp Fluids 57(188):1–16. https://doi.org/10.1007/s00348-016-2280-z

Peng D, Wang S, Liu Y (2016c) Fast PSP measurements of wall-pressure fluctuation in low speed flows: improvements using proper orthogonal decompostion. Exp Fluids. https://doi.org/10.1007/s00348-016-2130-z

Peng D, Jiao L, Yu Y, Liu Y, Oshio T, Kawakubo T, Yakushiji A (2017) Single-shot lifetime-based PSP and TSP measurements on turbocharger compressor blades. Exp Fluids 58(127):1–15. https://doi.org/10.1007/s00348-017-2416-9

Peng D, Chen J, Jiao L, Liu Y (2018a) A fast-responding semi-transparent pressure-sensitive paint based on through-hole anodized aluminum oxide membrane. Sens Actuators A-Phys 274:10–18. https://doi.org/10.1016/j.sna.2018.02.026

Peng D, Chen J, Yu Y, Jiao L, Liu Y (2018b) A novel laminated OLED-PSP system for measurement on moving surfaces. J Vis Jpn 21:215–223. https://doi.org/10.1007/s12650-017-0458-y

Peng D, Gu F, Li Y, Liu Y (2018c) A novel sprayable fast-responding pressure-sensitive paint based on mesoporous silicone dioxide particles. Sens Actuators A Phys 279:390–398. https://doi.org/10.1016/j.sna.2018.06.048

Peng D, Zhong Z, Cai T, Guo S, Zhao X, Liu Y (2018d) Integration of pressure-sensitive paint with persistent phosphor: a light-charged pressure-sensing system. Rev Sci Instr 89:085003. https://doi.org/10.1063/1.5041359

Peng D, Li Y, Jiao L, Liu Y (2019a) Challenges and countermeasures of fast psp applications for measurements on rotating blades. J Eng Thermophys. Accepted and under production

Peng D, Zhong Z, Gu F, Zhou W, Qi F, Liu Y (2019b) Pressure-sensitive paint with imprinted pattern for full-field endoscopic measurement using a color camera. Sens Actuators A Phys 290:28–35. https://doi.org/10.1016/j.sna.2019.03.009

Raffel M, Heineck JT (2014) Mirror-based image derotation for aerodynamic rotor measurements. AIAA J 52:1337–1341. https://doi.org/10.2514/1.J052836

Running CL, Sakaue H, Juliano TJ (2019) Hypersonic boundary-layer separation detection with pressure-sensitive paint for a cone at high angle of attack. Exp Fluids. https://doi.org/10.1007/s00348-018-2665-2

Ruyten W, Sellers M, Baker W (2009) Spatially nonuniform self-quenching of the pressure-sensitive paint PtTFPP/FIB. In: 47th AIAA aerospace sciences meeting, AIAA-2009-1660

Sakamura Y, Matsumoto M, Suzuki T (2005) High frame-rate imaging of surface pressure distribution using a porous pressure-sensitive paint. Meas Sci Technol 16:759–765

Sakamura Y, Suzuki T, Kawabata S (2015) Development and characterization of a pressuresensitive luminescent coating based on Pt(II)-porphyrin self-assembled monolayers. Meas Sci Technol 26(064002):1–8. https://doi.org/10.1088/0957-0233/26/6/064002

Sakaue H (1999) Porous pressure sensitive paints for aerodynamic applications. Purdue University, West Lafayette

Sakaue H, Ishii K (2010a) A dipping duration study for optimization of anodized-aluminum pressure-sensitive paint. Sensors 10:9799–9807

Sakaue H, Ishii K (2010b) Optimization of anodized-aluminum pressure-sensitive paint by controlling luminophore concentration. Sensors 10:6836–6847. https://doi.org/10.3390/s100706836

Sakaue H, Gregory JW, Sullivan JP (2002a) Porous pressure-sensitive paint for characterizing unsteady flowfields. AIAA J 40:1094–1098

Sakaue H, Matsumura S, Schneider SP, Sullivan JP (2002b) Anodized aluminum pressure sensitive paint for short duration testing. In: 22nd AIAA aerodynamic measurement technology and ground testing conference, AIAA-2002-2908

Sakaue H, Tabei T, Kameda M (2006) Hydrophobic monolayer coating on anodized aluminum pressure-sensitive paint. Sens Actuators B Chem 119:504–511

Sakaue H, Kakisako T, Ishikawa H (2011) Characterization and optimization of polymer-ceramic pressure-sensitive paint by controlling polymer content. Sensors 11:6967–6977

Sakaue H, Miyamoto K, Miyazaki T (2013a) A motion-capturing pressure-sensitive paint method. J Appl Phys 113:084901. https://doi.org/10.1063/1.4792761

Sakaue H, Morita K, Iijima Y, Sakamura Y (2013b) Response time scales of anodized-aluminum pressure-sensitive paints. Sens Actuators A Phys 199:74–79. https://doi.org/10.1016/j.sna.2013.04.040

Sano S, Yuuki T, Hyakutake T, Morita K, Sakaue H, Arai S, Matsumoto H, Michinobu T (2018) Temperature compensation of pressure-sensitive luminescent polymer sensors. Sens Actuators B Chem 255:1960–1966. https://doi.org/10.1016/j.snb.2017.08.221

Schairer ET (2002) Optimum thickness of pressure-sensitive paint for unsteady measurements. AIAA J 40:2312–2318

Schneider JJ, Engstler J, Budna KP, Teichert C, Franska S (2005) Free-standing, highly flexible, large area, nanoporous alumina membranes with complete through-hole pore morphology. Eur J Inorg Chem 2005:2352–2359. https://doi.org/10.1002/ejic.200401046

Schreivogel P, Paniagua G, Bottini H (2012) Pressure sensitive paint techniques for surface pressure measurements in supersonic flows. Exp Therm Fluid Sci 39:189–197. https://doi.org/10.1016/j.expthermflusci.2012.01.023

Schulz B, Klein C (2005) Light emitting surfaces of wind tunnel models for excitation of pressure sensitive paint. In: 21st international congress on instrumentation in aerospace simulation facilities. https://doi.org/10.1109/iciasf.2005.1569933

Scroggin AM, Slamovich EB, Crafton JW, Lachendo N, Sullivan JP (1999) Porous polymer/ceramic composites for luminescent-based temperature and pressure measurement. Mater Res Soc Proc 560:347–352

Shen Y, Clarke DR (2009) Effects of reducing atmosphere on the luminescence ofEu3+-doped yttria-stabilized zirconia sensor layers in thermal barriercoatings. J Am Ceram Soc 92:125–129. https://doi.org/10.1111/j.csz1551-2916.2008.02866.x

Singh M, Naughton JW, Yamashita T, Nagai H, Asai K (2011) Surface pressure and flow field behind an oscillating fence submerged in turbulent boundary layer. Exp Fluids 50:701–714. https://doi.org/10.1007/s00348-010-0977-y

Sugimoto T, Kitashima S, Numata D, Nagai H, Asai K (2012) Characterization of frequency response of pressure-sensitive paints. In: 50th AIAA aerospace sciences meeting including the new horizons forum and aerospace exposition, AIAA-2012-1185

Sugimoto T, Sugioka Y, Numata D, Nagai H, Asai K (2017) Characterization of frequency response of pressure-sensitive paints. AIAA J 55:1460–1464. https://doi.org/10.2514/1.J054985

Sugioka Y, Arakida K, Kasai M, Nonomura T, Asai K, Egami Y, Nakakita K (2018a) Evaluation of the characteristics and coating

film structure of polymer/ceramic pressure-sensitive paint. Sensors 18:4041. https://doi.org/10.3390/s18114041

Sugioka Y, Numata D, Asai K, Koike S, Nakakita K, Nakajima T (2018b) Polymer/ceramic pressure-sensitive paint with reduced roughness for unsteady measurement in transonic flow. AIAA J 56:2145–2156. https://doi.org/10.2514/1.J056304

Watkins AN, Leighty BD, Lipford WE, Wong OD, Oglesby DM, Ingram JL (2007) Development of a pressure sensitive paint system for measuring global surface pressures on rotorcraft Blades. In: 22nd international congress on instrumentation in aerospace simulation facilities. https://doi.org/10.1109/iciasf.2007.4380888

Watkins AN, Buck GM, Leighty BD, Lipford WE, Oglesby DM (2009) Using pressure- and temperature-sensitive paint on the aftbody of a capsule vehicle. AIAA J 47:821–829. https://doi.org/10.2514/1.37258

Watkins AN, Leighty BD, Lipford WE, Goodman KZ, Crafton J, Gregory JW (2016) Measuring surface pressures on rotor blades using pressure-sensitive paint. AIAA J 54:206–215. https://doi.org/10.2514/1.J054191

Weiss A, Geisler R, Schwermer T, Yorita D, Henne U, Klein C, Raffel M (2017) Single-shot pressure-sensitive paint lifetime measurements on fast rotating blades using an optimized double-shutter technique. Exp Fluids 58:120. https://doi.org/10.1007/s00348-017-2400-4

Wen X, Liu Y, Li Z, Chen Y, Peng D (2018) Data mining of a clean signal from highly noisy data based on compressed data fusion: a fast-responding pressure-sensitive paint application. Phys Fluids. https://doi.org/10.1063/1.5046681

Wong OD, Watkins AN, Ingram JL (2005) Pressure-sensitive paint measurements on 15% scale rotor blades in Hover. In: 35th AIAA fluid dynamics conference and exhibit, AIAA 2005-5008

Wong OD, Noonan KW, Watkins AN, Jenkins LN, Yao C (2010) Non-intrusive measurements of a four-bladed rotor in hover—a first look. In: American Helicopter Society Aeromechanics Specialists' Conference

Wong OD, Watkins AN, Goodman KZ, Crafton JW, Forlines A, Goss L, Gregory JW, Juliano TJ (2012) Blade tip pressure measurements using pressure sensitive paint. In: AHS 68th Annual Forum

Yang L, Zare-Behtash H, Erdem E, Kontis K (2012) Investigation of the double ramp in hypersonic flow using luminescent measurement systems. Exp Therm Fluid Sci 40:50–56. https://doi.org/10.1016/j.expthermflusci.2012.01.032

Yang L, Peng D, Shan X, Guo F, Liu Y, Zhao X, Xiao P (2018) "Oxygen quenching" in Eu-based thermographic phosphors: mechanism and potential application in oxygen/pressure sensing. Sens Actuators B-Chem 254:578–587. https://doi.org/10.1016/j.snb.2017.07.092

Yorita D, Nagai H, Asai K, Narumi T (2010) Unsteady PSP Technique for Measuring Naturally-Disturbed Periodic Phenomena. In: 48th AIAA Aerospace Sciences Meeting, AIAA-2010-307. https://doi.org/10.2514/6.2010-307

Yorita D, Henne U, Klein C (2017) Improvement of lifetime-based PSP technique for industrial wind tunnel tests. In: 55th AIAA aerospace sciences meeting, AIAA-2017-0703

Yorita D, Henne U, Klein C, Munekata M, Holst G (2019) Investigation of image-based lifetime PSP measurements with sinusoidal excitation light. In: AIAA Scitech 2019 Forum, AIAA-2019-0023

Zare-Behtash H, Yang L, Gongora-Orozco N, Kontis K, Jones A (2012) Anodized aluminium pressure sensitive paint: effect of paint application technique. Measurement 45:1902–1905. https://doi.org/10.1016/j.measurement.2012.03.015